

***PSEUDOMONAS* INTRODUCTION**

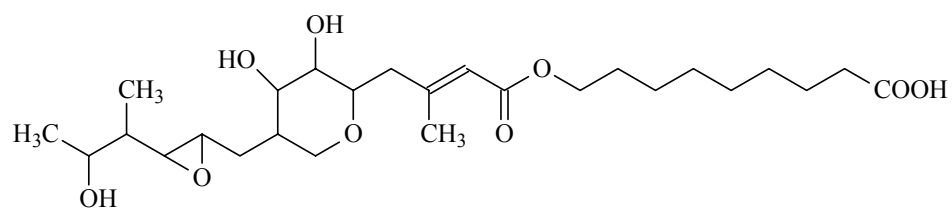
The discovery of the antibiotic penicillin by Alexander Fleming in 1928 eventually led to the formal treatment of disease with such microbial derived drugs (Wong, 2003). Penicillin is a natural product, and scientists have continued to search natural sources for new and effective medicinal compounds. Today almost half of the drugs used to treat disease have their roots in natural products (Dewick, 2002). Nevertheless, some pathogens still go untreated and others have developed resistance to known remedies, creating a constant need for new treatment methods.

As the demand for novel remedies continues, natural products are still an important source of new medicines. Natural products, sometimes known as secondary metabolites, are defined as compounds that do not appear to be essential to the life of the producing organism, but which may serve some other defensive, or anti-predatory role (Malik, 1980; DeLisa, 2002). Often these secondary metabolites are found to be organism specific and vary structurally under different growth conditions. In most cases, the biosynthetic building blocks for these secondary metabolites are derived from primary metabolites such as organic acids, amino acids, and carbohydrates leading to a wide range of structures. In microbes, secondary metabolite production is most often suppressed during the lag and exponential phases of growth and is greatest during the stationary phase when the highest concentration of primary metabolism side products is present (Malik, 1980).

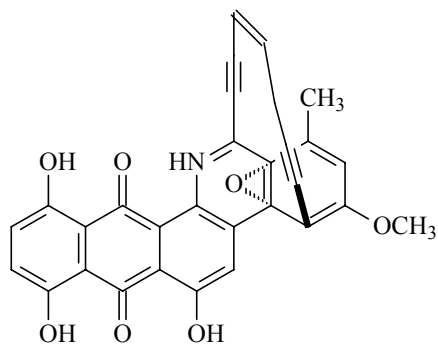
Based on their biosynthetic origin, secondary metabolites are classified into five main classes of natural products: polyketides, terpenes, shikimates, peptides, and

alkaloids. Each class has specific structural and biological characteristics and represent many of the beneficial products used in today's society. One of the most common types of natural products are the polyketides. These compounds are derived from simple organic acid units such as acetic acid, pyruvic acid, and butyric acid (Pfeifer, 2001; Hopwood). These acids are condensed on a large multifunctional enzyme called a polyketide synthase (PKS) to form β -keto chains that can be further modified (Simpson, 1995). Two examples of bioactive polyketides are pseudomonic acid A (**1**) (Figure 1A) and dynemycin (**2**) (Figure 1B). Pseudomonic acid A, produced by *Pseudomonas fluorescens*, is active against methicillin resistant *Staphylococcus aerus* (MRSA) infections while dynemycin, produced by *Micromonospora chersina*, acts as an anti-cancer agent (Mantle, 2001; Simpson, 1995). Further examples include the antibiotic tetracycline (**3**) (Figure 1C) and lovastatin (**4**) (Figure 1D), an effective cholesterol-lowering agent. Tetracycline is produced by *Streptomyces texas*, while lovastatin is produced by *Aspergillus terreus* (Brodersen, 2000).

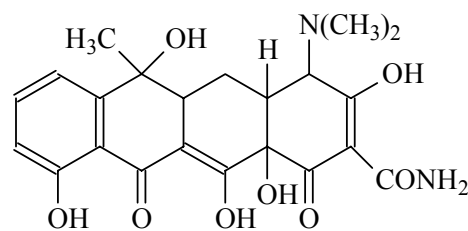
Another major class of natural products are the terpenes, which are derived from the isoprene moiety, a five-carbon unit. This isoprene unit is formed via the mevalonic acid (mevalonic pathway) or deoxyxylulose (deoxyxylulose pathway) and in most cases these units are assembled in a regular head-to-tail manner. This biosynthetic pathway can result in a variety of molecules called monoterpenes (C_{10}), sesquiterpene (C_{15}), diterpenes (C_{20}), triterpenes (C_{30}) and tetraterpenes (C_{40}). The sesterterpenes (C_{25}) are



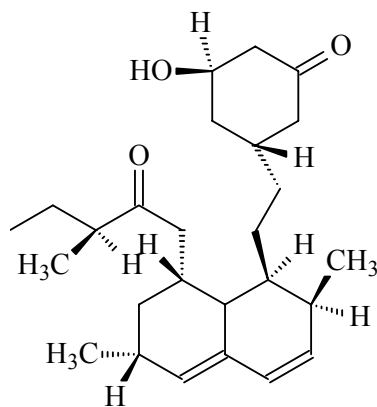
A: Pseudomonic Acid A (1)



B: Dynemycin (2)



C: Tetracycline (3)



D: Lovastatin (4)

Figure 1: Polyketide Secondary Metabolites from *Pseudomonas fluorescens*

- A) Pseudomonic Acid A (1)
- B) Dynemycin (2)
- C) Tetracycline (3)
- D) Lovastatin (4)

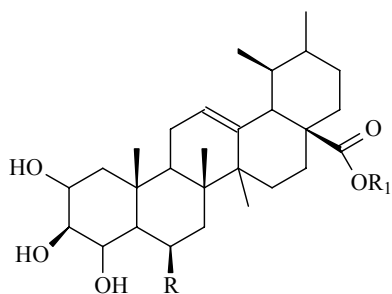
assembled from five isoprene units (Dewick, 2002) and two examples of this class that are produced by *Centella asiatica* (Jew, 2000) are asiatic acid (**5**) and madecassic acid (**6**) (Figure 2A). Each of these is used to decrease the wound area of skin necrosis induced by flesh burns (Cho, 2003).

The next group is known as the shikimates, which are ubiquitous in microorganisms and in plants. This group of compounds includes secondary metabolites containing aromatic amino acids, which in turn are derived from shikimic acid (Dewick, 2002). An example of a bioactive shikimate, is secoisolariciresinol (**7**) (Figure 2B). This molecule belongs to the lignan group of compounds and is commonly found in flax seeds. Secoisolariciresinol has been found to bind to human sex hormone binding globulin (SHBG), which is helpful in the treatment of benign prostatic hyperplasia (Eliasson, 2003).

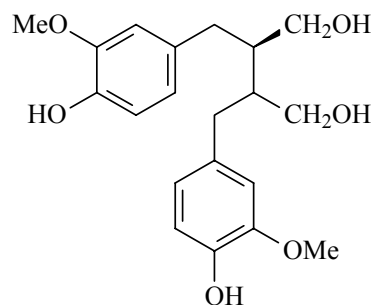
Another important group of natural products are the peptides, which are formed from a wide variety of protein and non-protein amino acid units. Typically these are oligomers of amino acids that are combined in either a linear or cyclic manner and are assembled by a process that does not require a ribosome (Dewick, 2002). Consequently, these compounds are called non-ribosomal peptides. Vancomycin (**8**) is typical of such a bioactive peptide (Figure 2C), and is produced by *Streptomyces orientalis*. This compound functions as an important therapeutic against multiple-resistant gram-positive bacteria and is of specific use against bacteria with ampicillan or methicillin resistance (Klare, 2003).

Lastly, the alkaloids are organic nitrogenous bases found mainly in plants, but are also found in animals and microorganisms to a lesser extent. Alkaloids contain one or more nitrogen atoms and can be of any hybridization. The main constituents of alkaloids are shikimic acid, acetate, and mevalonic acid (Dewick, 2002). Each of these constituents can be combined in a various manner to produce an alkaloid. A common example of an alkaloid produced by plants in the *Ephedra* genus is ephedrine (**9**) (Figure 2D), which is commonly used as a nasal decongestant or to treat bronchial asthma.

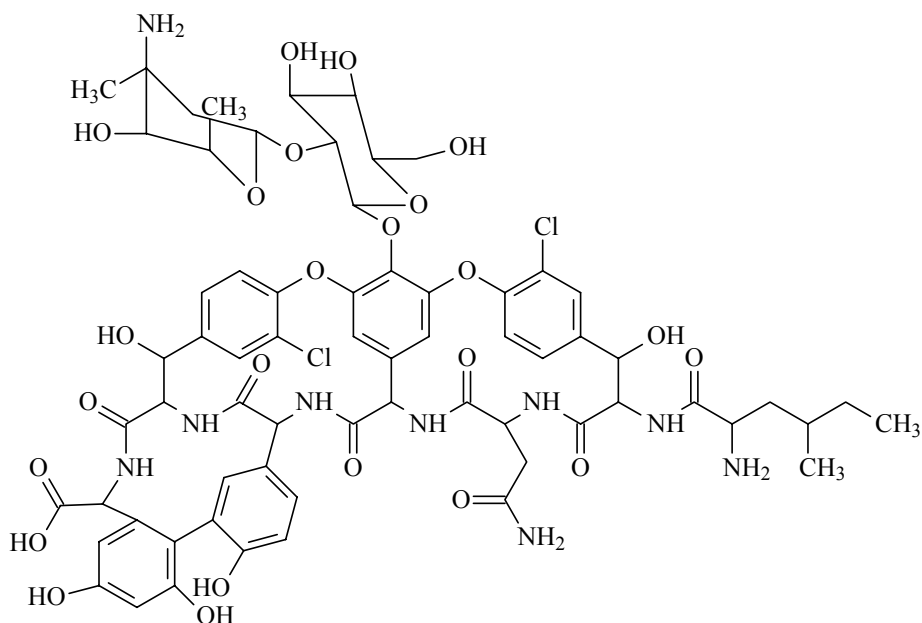
As the search for new drugs continues, scientists are exploring novel treatment methods. This is particularly true in the search for new anti-infectives, and one approach is to find molecules that interfere with the growth or virulence of infectious microorganisms. It was discovered that the marine bacterium *Vibrio fischeri* uses small molecules as a means of cell-to-cell communication to produce bioluminescence (Wolf-Watz, 2003). These molecules were named quorum sensing compounds or autoinducers. Quorum sensing is an environmental sensing system that allows bacteria to monitor their own population density. Specifically, bacteria produce autoinducers that allow the activation of certain transcription factors at high cell concentrations (Figure 3) (Loh, 2002) and such compounds have been found to regulate virulence, production of secondary metabolites, symbiosis, biofilm formation, and individual survival strategies (Bauer, 2002; Withers, 2001). A variety of different signaling compounds have been reported from different microbes (Figure 4). Typically gram-negative bacteria such as *P. fluorescens* use N-acyl homoserine lactones (AHLs), such as N-hexanoyl- HSL (**10**) and N-(3-oxo-octanoyl)- HSL (**11**), as cell-signaling



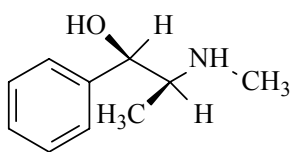
A: Asiatic Acid (5): R=H, R₁=H
 Madecassic Acid (6): R=H, R₁=OH



B: Secoisolariciresinol (7)



C: Vancomycin (8)



D: Ephedrine (9)

Figure 2: Further Examples of Bioactive Natural Products
 A) Asiatic Acid (5) and Madecassic Acid (6)
 B) Secoisolariciresinol (7)
 C) Vancomycin (8)
 D) Ephedrine (9)

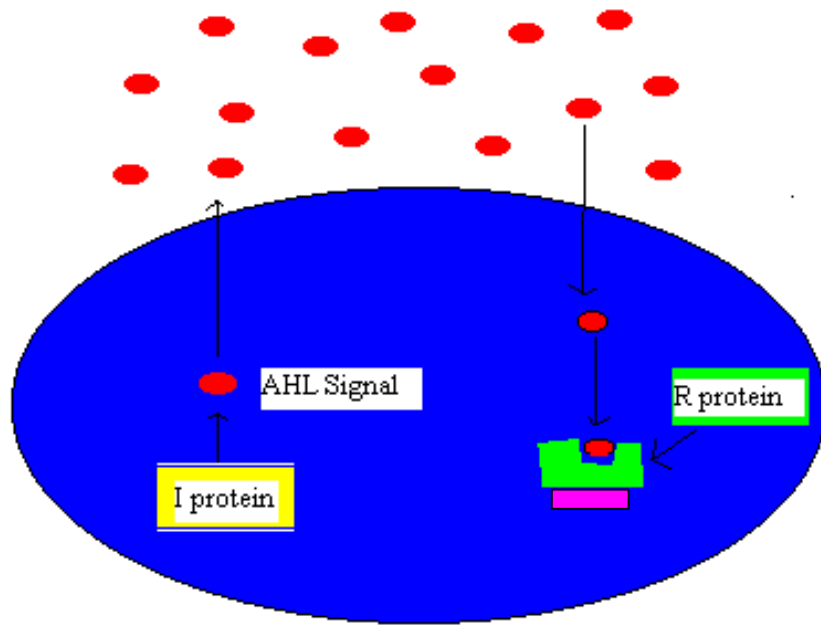
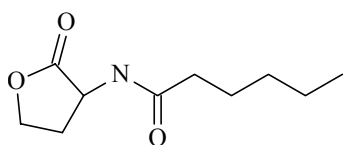
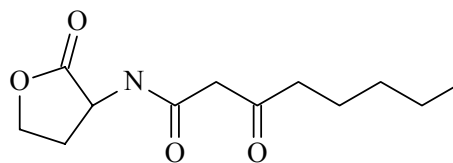


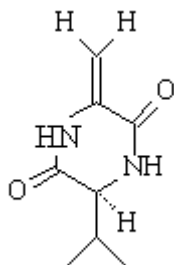
Figure 3: A simplified scheme for the AHL-mediated autoinduction by I and R proteins.



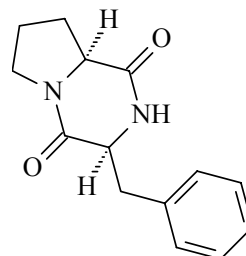
A: N-hexanoyl-L HSL (**10**)



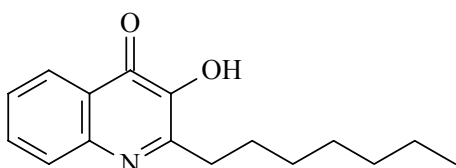
B: N-(3-oxo-octanoyl)-L-HSL (**11**)



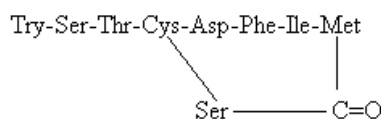
C: cyclo (Δ Ala-L-Val) (**12**)



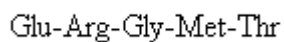
D: cyclo (L-Phe-L-Pro) (**13**)



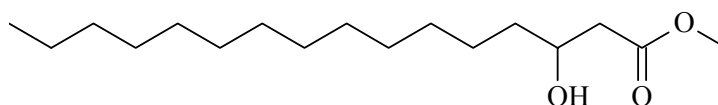
E: 2-heptyl-3-hydroxy-4-quinolone (**14**)



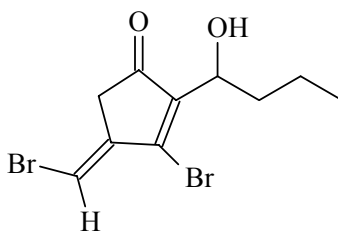
F: oligopeptide (**15**)



G: oligopeptide (**16**)



H: 3-hydroxypalmitic acid methyl ester (**17**)



I: 4-bromo-5(bromomethylene)-3-1'-hydroxybutyl-2(5H)-furanone (**18**)

Figure 4: Examples of Quorum Sensing Compounds

- A) N-hexanoyl-L HSL (**10**)
- B) N-(3-oxo-octanoyl)-L-HSL (**11**)
- C) cyclo (Δ Ala-L-Val) (**12**)
- D) cyclo (L-Phe-L-Pro) (**13**)
- E) 2-heptyl-3-hydroxy-4-quinolone (**14**)
- F) oligopeptide (**15**)
- G) oligopeptide (**16**)
- H) 3-hydroxypalmitic acid methyl ester (**17**)
- I) 4-bromo-5(bromomethylene)-3-1'-hydroxybutyl-2(5H)-furanone (**18**)

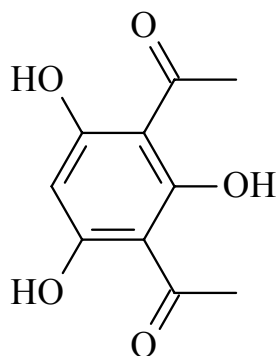
compounds, though other autoinducers are known to exist among the *Pseudomonas* genera and include diketopiperazines (DKPs) and *Pseudomonas* quinolone signal (PQS) (14) (Brelles-Marino, 2001; Holden, 1999). Besides the *Pseudomonads*, other organisms produce unique classes of cell-signaling molecules, and *Staphylococcus aureus* produces a group of oligopeptides such as those seen in Figure 4 (Donabedian, 2002; Schauder, 2001). On the other hand, a group of furanones produced by *Delisea pulchra* and *Xanthomonas campestris* have been found to act as antagonists to these known autoinducers (Whitehead, 2001).

The most common type of autoinducers are the AHLs, which all consist of a homoserine lactone ring containing a variable fatty acyl side chain (Schauder, 2001). The fatty acyl side chain can be four to fourteen carbons in length and may be saturated or unsaturated (Whitehead, 2001). Due to this variability in the length of the side chain, different methods of AHL transportation can operate. Short-chain acyl homoserine lactone (HSL) molecules are capable of passively diffusing across bacterial membranes, whereas long-chain acyl-HSLs are actively transported. Another site of variability in the side chain of AHLs is the presence of a hydroxyl or keto group at the C-3 position (Loh, 2002).

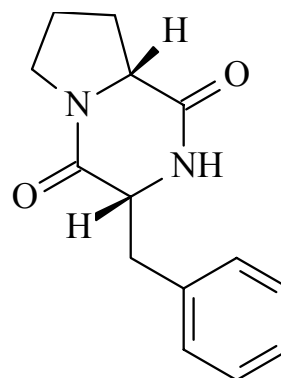
As the number of cells increase, AHLs accumulate until sufficient intracellular AHL is present to bind to the R protein, *luxR*, a transcriptional activator. The R protein is a 250 amino acid polypeptide and contains a carboxy-terminal region that is required for binding to a 20-basepair palindromic DNA sequence (*lux* box). Another structural feature of the R protein that is critical to its function, is the amino-terminus. This portion of the molecule is found to inhibit the *lux* box when AHL is unbound and contains the

actual AHL binding site (Loh, 2002). Specifically, the membrane-bound R protein receives incoming AHL signals, whereupon it undergoes a conformational change into the active form and after dimerization enters the cytoplasm to activate the *lux* box (Withers, 2001; Whitehead, 2001). The *lux* box is required for the *lux* gene expression and for the autoinduction response. This sequence of events is seen as a potential "therapeutic target for the design of small molecular antagonists capable of attenuating virulence through the blockade of bacterial cell-to-cell communication" (Williams, 2002).

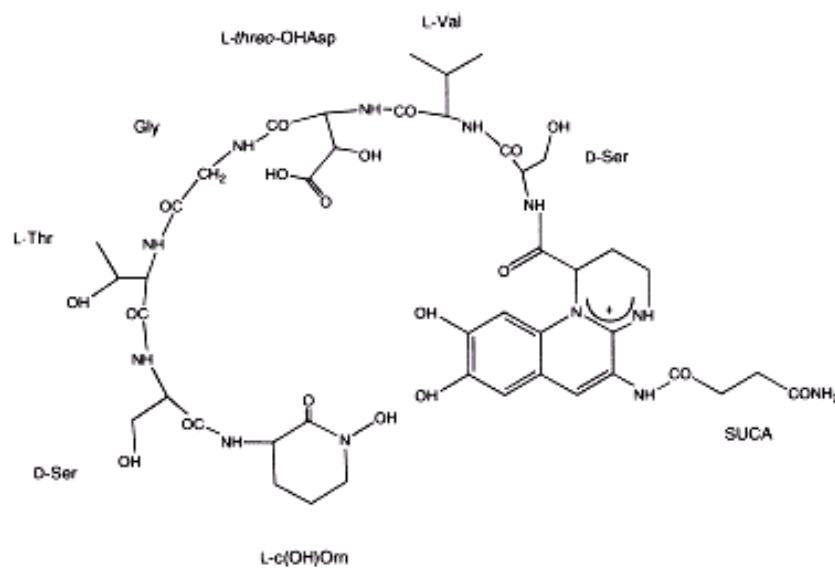
Pseudomonas fluorescens has been found to produce a wide variety of natural products or secondary metabolites (Fakhouri, 2001). Of most interest are compounds that act as antibiotics, antifungal agents, and cell-signaling compounds. The most common antibiotic produced by *P. fluorescens*, namely pseudomonic acid A (**1**), is used as a topical treatment for methicillin resistant *Staphylococcus aureus* (MRSA) infections of burn patients and other dermal infections. Another bioactive product is the antifungal agent 2,4-diacetylphloroglucinol (2,4-DAPG) (**19**) (Figure 5A). Not only is this compound active against soilborne fungal plant pathogens, but it has also been found to be active against *Staphylococcus* infections (Bangera, 1999). The diketopiperazine, (L-Phe-L-Pro) (**13**) (Figure 5B) is a common quorum sensing compound produced by *Pseudomonas fluorescens* and acts as an antagonist of 3-oxo-C6-HSL mediated induction of bioluminescence. This infers its ability to compete for the *LuxR*-binding site (Holden, 1999). Besides these bioactive agents, several compounds have been isolated that act as regulators, but do not act as anti-infectives. For example, exopolysaccharide (**20**) is a carbohydrate that is produced by a variety of *Pseudomonas fluorescens* strains (Osman,



A: 2,4-Diacetylphloroglucinol (**19**)



B: cyclo (L-Phe-L-Pro) (**13**)



C: Pyoverdinin (**21**)

Figure 5: Common Examples of Bioactive Compounds from *Pseudomonas fluorescens*

- A) 2,4-DAPG (**19**)
- B) cyclo (L-Phe-L-Pro) (**13**)
- C) Pyoverdinin (**21**)

1997). Also, a few compounds have been found to act as siderophores, compounds that chelate Fe^{3+} and transport this into the cell. The most common example of this is pyoverdinin (21) (Figure 5C), a fluorescent yellow-green peptide. This unusual linear peptide contains a dihydroxyquinoline chromophore that is linked to the peptide chain by an amide bond (Ongena, 2001; Mossialos, 2000; Philson, 1982). All of these compounds mentioned in this brief overview are examples of how natural products have benefited humankind and underscore the immense potential of natural products as medicinal therapeutics.

Due to the increasing need for effective medicinal agents, the study of *Pseudomonas fluorescens* as a source of bioactive secondary metabolites was pursued. As previously mentioned several compounds have been isolated from this bacterium, some of which act as antibacterial agents and quorum sensing molecules. Specifically, this study focused on the discovery of compounds that modulate the quorum sensing system of bacteria.

***PSEUDOMONAS* EXPERIMENTAL**

General

¹H NMR, ¹³C NMR, DEPT, COSY, HMQC, and TOCSY spectra were obtained in CDCl₃ using a Bruker 500 MHz (BBO probe). For gas chromatography/mass spectrometry an HP 5890 series II gas chromatograph (Hewlett Packard, USA) with a 30.0 m x 0.32 mm DB-5 cross-linked 5% phenyl-95% methyl polysiloxane column (film thickness-0.25 μm) was coupled with an HP 5871 series mass selective detector. Semi-preparative HPLC was performed using a Waters 1040 gradient controller coupled with a Waters UV detector using a Phenomenex Luna C₁₈ column (4.6 x 250 mm). Analytical HPLC was performed carried out on a Hewlett Packard 1100 using a Vydac Eclipse C₁₈ column (2.0 x 125 mm). Mass spectral data was collected on a Waters Micromass mass spectrometer using an electrospray probe. Open column chromatography was carried out using either Bakerbond Octadecyl (C₁₈) 40 μm Prep packing or Sephadex LH-20 packing in 30 x 1 cm glass columns. Initial separation was done on 10 g/60 ml ENVI-18 Sep-pak columns (Supleco). Thin layer chromatography (TLC) was performed using Macherey-Nagel Polygram Sil/UV plates, and visualization with vanillin/H₂SO₄ spray (Appendix 1). All chemicals were HPLC grade (Fisher or Aldrich). Concentration under reduced pressure was performed using a Buchi rotoevaporator modal R3000 or using a Savant speedvac model SC210A. Bioassay agar was *P. fluorescens* agar (Difco) and the bioassay disks were from S & S Biopath, Inc. (0.25" diameter).

Pseudomonas fluorescens Cultures

Pseudomonas fluorescens NCIB 10586 was maintained in both the labs of Dr. Sizemore and Dr. Wright. NCIB 10586 was maintained on both *Pseudomonas*

fluorescens agar supplemented with ampicillin (100 μ g/ml) and brain heart infusion agar. All slants were stored at 15° C and slants were transferred every three weeks.

A loopful of *Pseudomonas fluorescens* was used to inoculate 25 ml LB broth. This was placed on a stir plate at 25°C and stirred at a medium speed for 24 hours. Then 25 ml mupirocin production medium (MPM) was inoculated with 1.25 ml seed culture. In a 4 L Erlenmeyer flask, 2 L MPM was grown at 25°C on a stir plate for 48 hours.

The MPM consisted of yeast extract (2.3 %), Na₂HPO₄ (2.6%), KH₂PO₄ (2.4 %), (NH₄)₂SO₄ (5.0 %), glucose (1.1 %), in distilled water. Sterilization was at 121°C for 20 minutes. Media was allowed to cool for at least 24 hours before inoculation.

Bioassay Procedure

A loopful of either *E. coli* or *B. subtilis* was placed in a corresponding vial of LB broth and was incubated at 37°C for 24 hours. After incubation, 30 μ l of bacterial broth was placed on each agar plate. The broth was spread evenly on the plate using sterile techniques. Each fraction to be tested was dissolved in a small amount of methanol (MeOH) and an aliquot (20 μ l) of each fraction was placed on a bioassay disk. Each disk was allowed to dry for three hours and each disk was placed on the inoculated agar plates upside down. The plates were then incubated for 24 hours at 37°C. Zones of inhibition were monitored.

Cell-Signaling Assay

All fractions tested for cell-signaling activity were carried out in the Pesci lab at Eastern Carolina University School of Medicine. Activity was determined using a standard β -galactosidase assay where the activity was measured in Miller units:

$$\beta\text{-gal activity (Miller Units)} = \frac{1000 \times A_{420}}{\text{time (min)} \times \text{volume (ml)} \times A_{660}}$$

Extraction and Isolation

An outline of a typical isolation procedure is seen in Figure 6. Cells of *P. fluorescens* NCIB 10586, were pelleted by centrifugation (8,000 x g for 12 minutes). The acidified broth (pH \approx 4.0) was then extracted with isobutyl methyl ketone (IBMK) and the organic extract was concentrated under reduced pressure. The dried extract (368 mg/26 L) was run on a Sep-pak column and eluted from 20%-100% MeOH (10% gradient steps). Ten fractions were collected and tested for cell-signaling activity and also run on a TLC plate in CHCl₃:MeOH (9:1) (vanillin/H₂SO₄ spray; Appendix 1). Fraction four was found to be of interest and was further purified using a Bakerbond C₁₈ column and elution from 40-60% aqueous MeOH in 5% increments, then 60%-100% MeOH in 20% increments, followed by a final elution with one column volume of 100% MeOH. Fractions (1 mL) were collected and combined based on TLC analysis. The third group of fractions was further purified using an LH-20 column, 0.5 ml fractions were collected and combined based on TLC. The second group of LH-20 fractions (23 mg) purified by semi-preparative HPLC (Bakerbond C₁₈) and isocratic elution with 53% aqueous ACN (UV monitoring at 214 nm and 254 nm). Six peaks were collected: peaks three, four, and six were then completely purified using analytical HPLC with an elution system from 20-90% aqueous ACN over 30 minutes (UV monitoring at 214 nm and 254 nm). Peak three and four were found to correlate to an unknown metabolite (**25**) and indole-3-carboxylic

acid (**24**), respectively. Peak six was found to contain two compounds, tryptophol (**22**) and indole-3-aldehyde (**23**).

This procedure was repeated three times (total 78 L of culture) to yield tryptophol (**22**, 1.7 mg), indole-3-aldehyde (**23**, 0.73 mg), indole-3-carboxylic acid (**24**, 1.2 mg), and an unknown metabolite (**25**, 0.42 mg). UV spectra of these compounds were collected (Figure 7) and each compound was then tested for cell-signaling activity following the standard procedure (Table 1).

^1H , ^{13}C , DEPT, HMQC, COSY, and TOCSY NMR spectra were collected for **22** and can be seen in Appendix 2-6. ^1H NMR data was collected on **23**, **24**, and **25** (Figure 8). Each compound was also run on the LC/MS from 20-90% aqueous acetonitrile/3 mM formic acid over 30 minutes (flow rate: 0.4 ml/min). Electrospray spectra in the positive and negative mode were collected. The specific mass spectrometer conditions can be found in Appendix 7. The mass spectra of **22**, **23**, **24**, and **25** are shown in Appendix 8, Appendix 9, Appendix 10, and Appendix 11, respectively. GC/MS spectra were collected by running each of these isolates from 120°C-260°C at a temperature gradient of 20°C/14 seconds. All this data was compiled to elucidate the structures of tryptophol (**22**), indole-3-aldehyde (**23**), and indole-3-carboxylic acid (**24**).

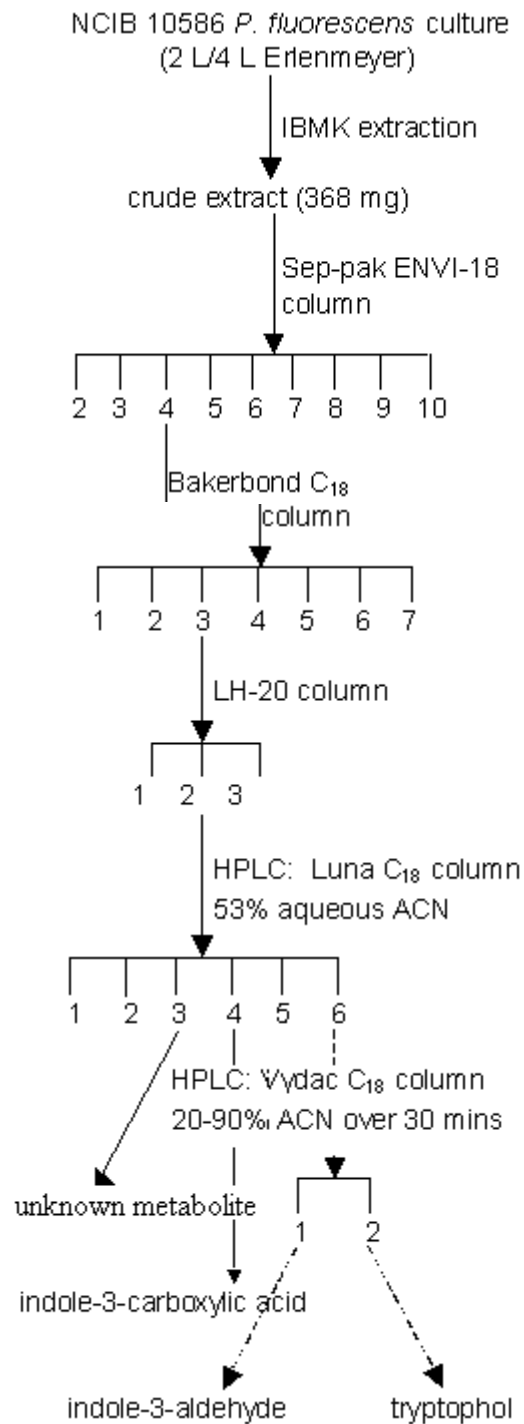
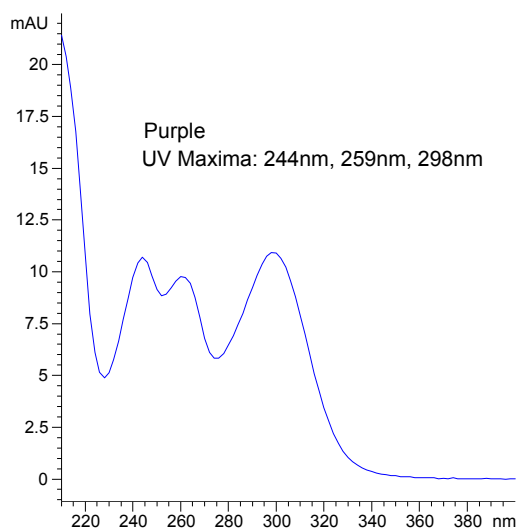
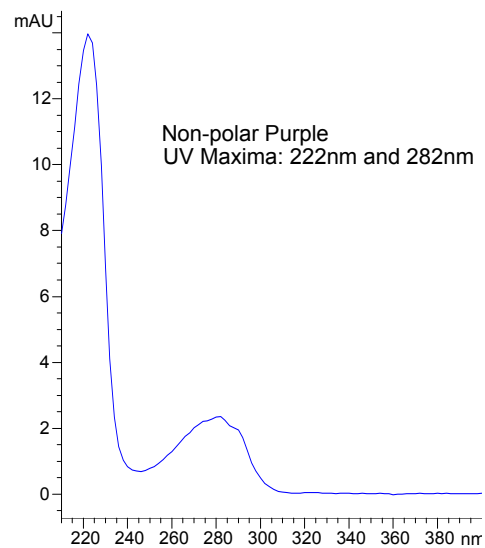


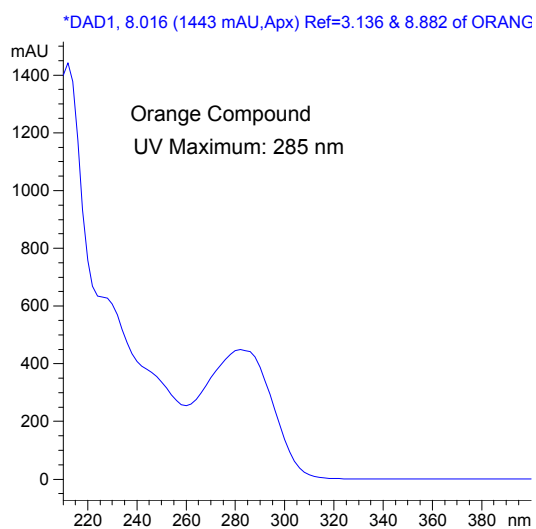
Figure 6: Isolation of Tryptophol (**22**), indole-3-aldehyde (**23**), indole-3-carboxylic acid (**24**), and unknown metabolite (**25**)



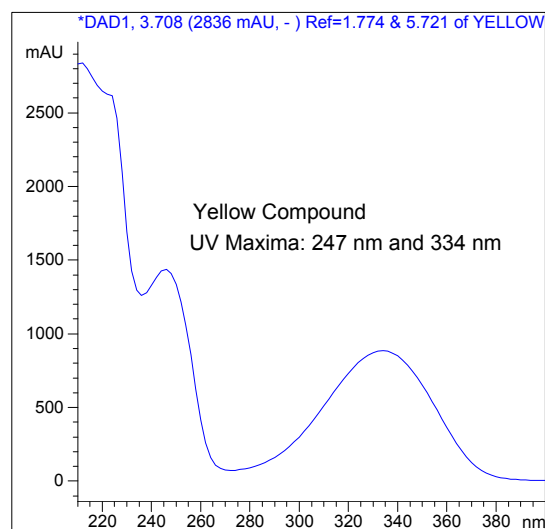
A) indole-3-aldehyde (**23**)



B) Tryptophol (**22**)



C) indole-3-carboxylic acid (**24**)



D) Unknown Metabolite (**25**)

Figure 7: UV Spectra of Indole Derivatives
 A) indole-3-aldehyde (**23**)
 B) Tryptophol (**22**)
 C) indole-3-carboxylic acid (**24**)
 D) Unknown Metabolite (**25**)

Sample Name	Mass (microgram)	B-galactosidase Activity (Miller Units)	
		Sample	Control
indole-3-aldehyde	24	528	336
Tryptophol	25	841	336
indole-3-carboxylic acid	24	503	336
Unknown Metabolite	32	407	405

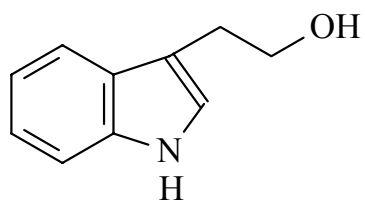
Table 1: β -galactosidase Cell-Signaling Assay Results

***PSEUDOMONAS* RESULTS**

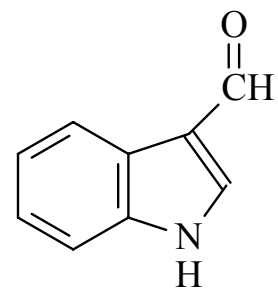
Following extraction and fractionation of *Pseudomonas fluorescens* cultures several fractions were found to possess cell signaling activity. This large scale extraction of culture (78 L) yielded crude extract (1.1 g) which upon purification by various chromatography steps, four pure compounds were isolated. These pure compounds were identified as tryptophol (**22**), indole-3-aldehyde (**23**), and indole-3-carboxylic acid (**24**) (Figure 9) and were found to be active in the cell-signaling assay (Table 1).

Characterization of Secondary Metabolites from *Pseudomonas fluorescens*

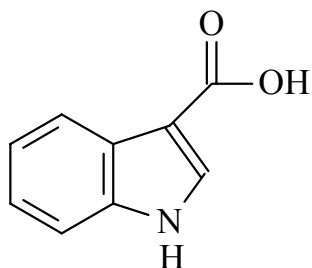
Compound **22**, tryptophol was obtained as a white powder and displayed UV maxima at 222 nm and 282 nm in acetonitrile, which is consistent with an indole moiety (Gilchrist, Andonovski). The positive ion electrospray MS showed an $[M+H]^+$ at m/z 162.2 consistent with the molecular formula of $C_{10}H_{11}NO$ for tryptophol (**22**). Fragments in the positive ion ESIMS at m/z values of 144.1, 130.1, 117.1, and 103.1 were observed at variable cone voltages, and are consistent to fragments of **22** as shown in Figure 10. Of specific interest is the ESIMS+ fragment at m/z of 117.1, which corresponds to the parent indole group ($C_8H_6N^+$) and the m/z of 144.1 indicating the loss of water. By GC/MS, several corresponding peaks were present at m/z 161, 130, 117, and 103, further supporting the LC/MS data. Based on previously published H^1 and C^{13} NMR spectra, the values found here (Figure 11) are consistent with the proposed structure. The H^1 NMR displayed the presence of six aromatic protons consisting of δ 8.05 (1H, s, broad), 7.65 (1H, d, $J=7.76$ Hz), 7.40 (1H, d, $J=8.00$ Hz), 7.24 (1H, t, $J=7.52$ Hz), 7.16 (1H, t, $J=7.29$ Hz), and 7.07 (1H, s), thereby indicating the presence of either a phenol or an aromatic



A: Compound **22**, Tryptophol



B: Compound **23**, indole-3-aldehyde



C: Compound **24**, indole-3-carboxylic acid

Figure 9: Structures of *Pseudomonas fluorescens* Isolates

- A) Tryptophol (**22**)
- B) indole-3-aldehyde (**23**)
- C) indole-3-carboxylic acid (**24**)

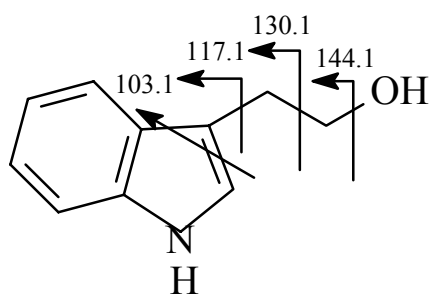
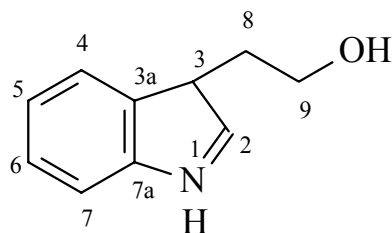


Figure 10: Mass Spectrum Fragmentation of Compound **22**, Tryptophol



Position	H ¹ Chemical Shift	J (Hz)	C ¹³ Chemical Shift	H ¹ Multiplicity	H ¹ Integration
1	8.05			s	1
2	7.07		122.43	s	1
4	7.40	7.29	111.19	d	1
5	7.24	7.52	122.25	t	1
6	7.16	8.00	119.52	t	1
7	7.65	7.76	118.86	d	1
8	3.08	6.07	28.78	t	2
9	3.95	6.16	62.64	t	2
OH	1.57			s	1

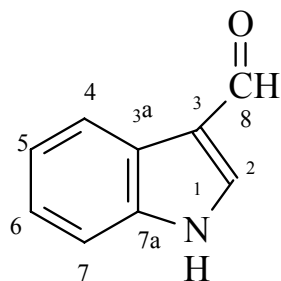
Figure 11: Compiled NMR (CDCl₃) Data for Compound **22**, Tryptophol

amine group due to the broad singlet and the presence of a two ring system due to the splitting pattern. Further ^1H NMR data included the presence of protons at δ 3.95 (2H, t, $J=6.16$ Hz) and 3.08 (2H, t, $J=6.07$ Hz), indicating the presence an alkyl chain. TOCSY NMR revealed three spin systems to be present, where the protons at δ 8.05 and 7.07 composed spin system one, protons at δ 7.65, 7.40, 7.24, and 7.16 composed spin system two, and protons at δ 3.95 and 3.08 composed the final spin system. HMQC correlations in conjunction with DEPT NMR data revealed that the protons at δ 3.95 and 3.08 are attached to carbons at δ 62.64 (CH_2) and 28.78 (CH_2), respectively, and the HMQC NMR data was established that the protons at δ 8.05 and 1.57 are not attached to carbons, indicating the possibility of attachment to either oxygen or nitrogen. COSY correlations showed the following couplings δ 7.16/ δ 7.65. Further couplings exist between δ 7.24/ δ 7.40 and δ 7.24/ δ 7.16. Based on all the structural data collected, compound **22** was identified as tryptophol.

Compound **23**, indole-3-aldehyde, was obtained as a white powder, but the amount of material isolated was not enough to carry out a complete spectral analysis. However the identification of the closely related compound, tryptophol (**22**) allowed a correlation between the two compounds to be established. The UV spectrum of **23** in aqueous acetonitrile had UV maxima at 244 nm, 259 nm, and 298 nm. When these UV maxima are compared to those for a typical indole the values are slightly higher than expected, 244 nm and 298 nm. This would indicate extended conjugation within the system causing the maxima to shift to longer wavelengths. Also, the presence of a third UV maximum, 259 nm, revealed the presence of a carbonyl group, which is typically

found around 270 nm caused by the $n-\pi^*$ transition (Crews, 1998). In the positive ion ESIMS, a peak corresponding to $[M+H]^+$ was observed at m/z 146.1 consistent with a molecular formula of C_9H_7NO . Fragments in the positive ion ESIMS showed $[M+H]^+$ peaks at m/z values of 117.1 ($C_8H_6N^+$) and 103.1 ($C_6H_5N^+$) at variable cone voltages. Both of these fragments were also present in the tryptophol (**22**) and correspond to fragmentation of the base indole structure. The H^1 NMR (Figure 12) displayed the presence of six aromatic protons just as was found in **22**, consisting of δ 8.70 (1H, s, broad), 8.35 (1H, d, $J=3.15$), 7.88 (1H, d, $J=2.90$), 7.47 (1H, t, $J=4.06$), 7.36 (1H, t, $J=3.93$), 7.07 (1H, s). This pattern of aromatic splitting was almost identical with that for **22** further supporting the close structural similarity between the two molecules. Significantly the H^1 NMR data revealed a proton resonance at δ 10.12 consistent with the presence of an aldehyde group. Despite the lack of further NMR data due to the lack of material, compound **23** was identified as indole-3-aldehyde.

Compound **24**, indole-3-carboxylic acid, was also obtained as a white powder. Once again the small amounts of compound isolated (0.68 mg) precluded full structural analysis, but again based on the tryptophol spectral information the structure of the closely related compound **24** could be deduced. The UV spectrum of indole-3-carboxylic acid (**24**) in aqueous acetonitrile/0.1% TFA had UV maxima at 210 nm, 228 nm and 285 nm, where the later two maxima are within the typical range for an indole group. The presence of a UV maximum at 210 nm is indicative of a carboxylic acid carbonyl group, which is typically around 200 nm (Crews, 1998). In positive ion ESIMS, a peak corresponding to $[M+H]^+$ was observed at m/z 162.2. Fragment peaks present in the

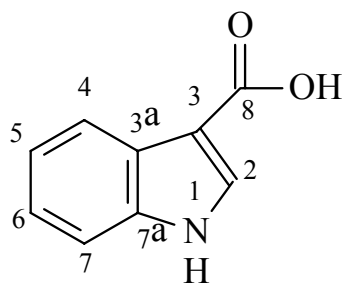


Position	H ¹ Chemical Shift	J (Hz)	H ¹ Multiplicity	H ¹ Integration
1	8.70		s	1
2	7.07		s	1
4	8.35	3.15	d	1
5	7.36	3.93	t	1
6	7.47	4.06	t	1
7	7.88	2.90	d	1
8	10.10		s	1

Figure 12: H¹ NMR (CDCl₃) Data for Compound 23, indole-3-aldehyde

positive ion ESIMS corresponding to $[M+H]^+$ were observed at m/z 144.1, 117.1, and 103.1, consistent with an indole structure. The 1H NMR (Figure 13) showed the presence of six aromatic protons at δ 8.63 (1H, s, broad), 8.24 (1H, d, $J=3.80$), 8.02 (1H, d, $J=2.90$), 7.47 (1H, t, $J=4.56$), 7.33 (1H, t, $J=4.53$) and 7.07 (1H, s), once again almost identical with the pattern obtained for compound **22**. The 1H NMR data also contained exchangeable singlet at δ 12.16, indicating the presence of a carboxylic acid group. While this data alone was not enough to finalize the structure, but the data strongly suggests that compound **24** is indole-3-carboxylic acid. Also, this was confirmed by comparison with a known standard.

An unknown metabolite (**25**) was obtained as a yellow-white powder. The UV spectrum of **25** in aqueous acetonitrile had UV maxima at 247 nm and 334 nm. In positive ion ESIMS a peak corresponding to an $[M+H]^+$ had an m/z 138.1 suggesting a possible molecular formula of $C_8H_{11}NO$. Fragments in positive ion ESIMS corresponding to $[M+H]^+$ peaks were present at m/z 120, 106, and 103, indicating the loss of water followed by the loss of a $-CH_2$ group. The last fragment, m/z 103.1, could be accounted for by the loss of ammonia and the loss of water. An important feature of the MS data is the lack of a mass fragment at m/z 117.1 characteristic of an indole moiety GC/MS data collected showed mass fragments at 137, 119, and 92; confirming the molecular weight of the compound, but did not provide any further structural data. The 1H NMR displayed the presence of four aromatic protons at δ 7.90 (1H, d, $J=8.47$), 7.33 (1H, s), 7.25 (1H, s), and 6.69 (1H, d, $J=7.59$) as well as two low field protons at δ 1.46 (1H, s) and 1.28 (3H, s). The NMR data was not consistent with an indole ring system and could not be



Position	H ¹ Chemical Shift	J (Hz)	H ¹ Multiplicity	H ¹ Integration
1	8.63		s	1
2	7.07		s	1
4	8.24	3.80	d	1
5	7.33	4.53	t	1
6	7.47	4.56	t	1
7	8.02	2.90	d	1
8	12.16		s	1

Figure 13: H¹ NMR (CDCl₃) Data for Compound **24**, indole-3-carboxylic acid

correlated with the mass spectral data that was collected, leading to the inability to deduce the structure of compound **25**.

Cell-Signaling Activity of *Pseudomonas fluorescens* Isolates

Pseudomonas fluorescens has been shown to produce several autoinducers, a few of which are also common in *Pseudomonas aeruginosa* strains (El-Sayed, 2001). Interestingly, none of these commonly found autoinducers were detected in the LC/MS analysis of the culture extract fractions, but based on the β -galactosidase assay carried out at Eastern Carolina University School of Medicine several culture extract fractions showed activity. Upon isolation, **22**, **23**, and **24** were shown to have cell-signaling activity, where the activity is based on the relative absorbance of ONP due to the production of β -galactosidase in *Pseudomonas aeruginosa* cells. Among these three compounds, tryptophol (**22**) had nearly twice the cell-signaling activity, 841 Miller units, as indole-3-aldehyde (**23**)(528 Miller units) and indole-3-carboxylic acid (**24**)(503 Miller units). The control was 336 Miller units. Based on the moles of compound that was tested, molar activity was found to be 5.43×10^9 activity/mol, 3.18×10^9 activity/mol, and 3.38×10^9 activity/mol for **22**, **23**, and **24**, respectively. Comparing these activities based on their molar values, tryptophol (**22**) is 41% more active than indole-3-aldehyde (**23**) and 38% more active than indole-3-carboxylic acid (**24**).

Bioactivity of *Pseudomonas fluorescens* Isolates

In previous studies, tryptophol has been found to act as an antifungal agent against *Mortierella ramannianus* (Li, 1994), but no reported studies have been carried out on the antibacterial activity of this molecule or the other compounds isolated within this

study. From the bioassay none of the isolated compounds were found to have any bioactivity.

Pseudomonic Acid A (**1**) Detection

Surprisingly, pseudomonic acid A was not found in any of the cultures of *P. fluorescens* although numerous growths were tried. The search for **1** was performed using TLC comparisons with a standard sample, but this posed problems since there were many compounds that had a similar R_f value (0.24-0.30) and had the same purple-gray color when sprayed with vanillin. Further analysis was carried out after the first purification step, and each group of fractions was tested using a standard HPLC/UV procedure developed using the pseudomonic acid A (**1**) standard and retention times were compared. Based on these tests, several fractions could have contained pseudomonic acid A (**1**) peak present, but absolute confirmation was not possible due to the complexity of the samples. Finally, LC/MS was employed to various fractions. From three growths, using a procedure developed for the pseudomonic acid A (**1**) standard. Once again, pseudomonic acid A (**1**) could not be detected in any sample.

PSEUDOMONAS DISCUSSION

Three indole derivatives were isolated from *Pseudomonas fluorescens* broth cultures and were found to exhibit cell-signaling activity. Following structural characterization, these derivatives were identified as tryptophol (**22**), indole-3-aldehyde (**23**), and indole-3-carboxylic acid (**24**). Each of these compounds has previously been isolated from a diverse group of organisms, although none have been associated with cell signaling in bacteria.

The most active cell-signaling compound was found to be tryptophol (**22**), a known antifungal and auxin agent, previously isolated from *Aspergillus niger*, *Balansia epichloe*, *Ircinia spinulosa*, *Pseudomonas fluorescens* (strain KGPP 937), and *Rhizobium* sp (Ten, 2000; Lebuhn, 1997). These sources included plant-associated bacteria, a marine sponge, and fungi. The specific means of auxin action of tryptophol (TOL) (**22**) results from its uptake by plants and the conversion to the active phytohormone, indole-3-acetic acid (IAA) (**31**), by plant TOL-oxidase and oxygen. While IAA is the active auxin present in most bacterial cultures, auxin production shifts to **22** in an O₂⁻ deficient system, possibly due to an increased microbial activity in soil microhabitats (Lebuhn, 1997). These attributes coincide with the data collected within this study; the ability of tryptophol (**22**) to act a cell-signaling molecule indicates its role as an auxin-like compound. Whether tryptophol (**22**) acts as a cell-signal for the producing bacteria or for the plants is unknown, but based on the fact that tryptophol (**22**) has been found to act as an auxin it is believed that tryptophol causes a cell-signaling cascade within the plant cell system. The possible use of tryptophol (**22**) as a precursor for **31** leads to many possibilities for enhanced crop growth. A further advantage to the supplementation of

plants with tryptophol (**22**) rather than the direct use of IAA is the greater rate of uptake of tryptophol (**22**) by the plant cell (Lebuhn, 1997).

The other two less active compounds, indole-3-aldehyde (**23**) and indole-3-carboxylic acid (**24**) were found to have virtually identical cell-signaling activity. To date, neither of these compounds has been found in plant-associated bacteria and only minimal information has been recorded about their ability to act as auxin-like compounds or to exhibit any other forms of bioactivity. Previous isolation of **23** has been found from a red alga *Chondira* sp. and also a *Halichondria* sp., a marine sponge. While **24** has been isolated from fungi, *Aporpium caryae*. While produced by different organisms, the structural similarity of these compounds provide an interesting opportunity to explore a structure-activity study. While the indole moiety appears in all of the elucidated structures, the side chain of each is variable. A variation in side chain length also affects the signaling activity of the AHL quorum sensing compounds. In the case of the indole derivatives it appears that a smaller side chain results in decreased activity, possibly as a result of decreased affinity for the *luxR* type receptor, therefore decreasing the induction level, but not losing it entirely. While less active than tryptophol, these compounds may allow the possible application as bacterial control agents. Since tryptophol (**22**) has been found to lyse human red blood cells and induce a sleep-like state, these derivatives may have reduced negative side effects (Seed, 1978). If these side effects can be eliminated, the use of **23** and **24** as therapeutic agents holds great merit. Consequentially, it would be interesting to perform toxicology studies to access their potential as medicinal agents.

The unknown metabolite, compound **25** did not demonstrate cell-signaling activity. The NMR and MS data are conflicting, and the molecular data is not consistent

with an indole structure, in line with the idea that the indole moiety is necessary for cell signaling activity.

As was noted earlier, the production of pseudomonic acid by *Pseudomonas fluorescens* has been found to be regulated by a quorum sensing system (El-Sayed, 2001). Along with these findings, it is also known that when pseudomonic acid is produced, two common AHLs (C10HSL (**29**) and C6HSL (**30**)) are present in organic extracts (El-Sayed, 2001). While within this study neither **29** or **30** were detected by LC/MS, which could account for the absence of pseudomonic acid in these cultures. This hypothesis could be examined by the addition of these AHLs to the growth media with the aim of activating pseudomonic acid (**1**) production.

***PSEUDOMONAS* CONCLUSIONS**

Within this study, four secondary metabolites from *Pseudomonas fluorescens* were isolated and three of these were identified: tryptophol (indole-3-ethanol) (**22**), indole-3-aldehyde (**23**), indole-3-carboxylic acid (**24**). The fourth metabolites could not be characterized based on current data. Each of the characterized indole derivatives was found to possess cell-signaling activity based on the standard β -galactosidase assay, while the unknown metabolite was inactive. Based on the results found here, the lack of cell-signaling activity of the unknown metabolite may be due to the incomplete formation of the indole ring system, but full structure elucidation is still needed.

There may be biotechnological or therapeutic potential for these compounds or their derivatives due to their ability to affect cell-signaling activity.

Finally, while the new quorum sensing compounds were found in cultures of *Pseudomonas fluorescens*, the common signaling compounds required in the production of pseudomonic acid (**1**) were not present. This could explain the absence of this compound in culture of *P. fluorescens* that were examined.

MICROCYSTIN INTRODUCTION

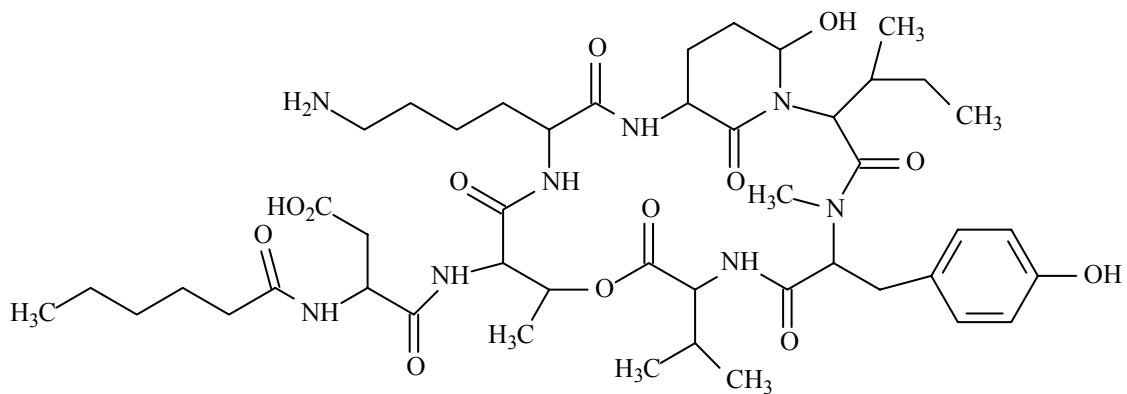
According to a variety of health studies, the average person should consume eight cups of water a day, which translates into 182 gallons of water per year. For this reason it is necessary to have a set of drinking water standards to ensure the safety of drinking water supplies. In 1974, the Safe Drinking Water Act (SDWA, 2003) was established in order to “protect public health from [water] source to tap” (EPA, 2003). The overall purpose of the SDWA was to set national health-based standards for drinking water to protect against both naturally occurring and man-made contaminants that may be present (EPA, 2003). Upon the enactment of the SDWA, many amendments have been made. One that has not yet been added is the establishment of maximum consumption levels of several caustic natural water toxins, such as the microcystins produced by cyanobacteria. Currently only Australia, Canada, and Great Britain have moved to establish maximum acceptable levels for microcystins in drinking water supplies (HAB, 2002). As of 1994, all of these countries have now set the maximum acceptable level to 0.1 µg/L of microcystins in drinking water (Rivasseau, 1998). From the lead of these countries and current toxicity studies, it has been established that there is a health risk at hand and action needs to be taken to monitor the consumption of these toxins.

Cyanobacteria or blue-green algae are photosynthetic bacteria that grow in both eutrophic freshwater and brackish water environments (Ohtake, 1989). These eubacteria are unicellular and can form massive colonies called blooms. Although structurally related to bacteria, blue-green algae have the ability to photosynthesize, and contain chlorophyll A and accessory pigments such as phycocyanin, which results in their blue-

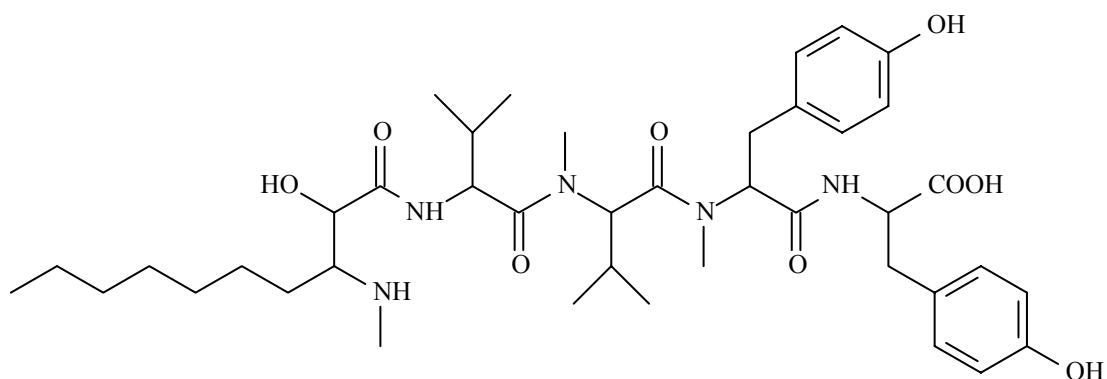
green coloration. These organisms thrive in eutrophic conditions and produce a range of secondary metabolites including toxins.

Although not all cyanobacteria cause threats to the environment, approximately 50-70% are found to be toxic (Fogg, 1998). At least 19 species belonging to nine genera have been shown to be toxin producers, and among these one of the major toxin producers is the *Microcystis* genera (HAB, 2002). Geographically, *Microcystis aeruginosa* is the most widely distributed among the toxic cyanobacteria, and consequently much emphasis has been placed on the study of this organism. *M. aeruginosa* grows in colonies, as do many other species, forming spherical, ellipsoidal, or irregularly lobed blooms. These colonies can be up to several centimeters in diameter where the individual cells are spherical and about 4.5 μm in diameter (HAB, 2002).

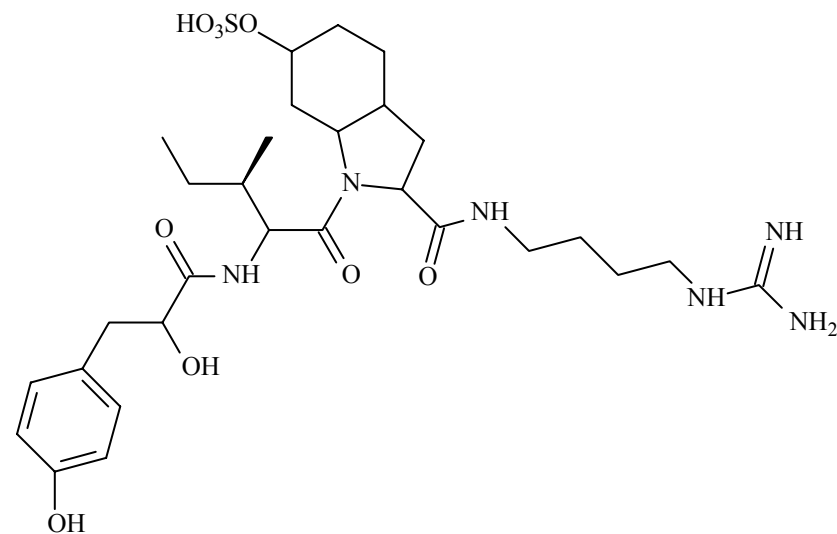
A number of toxins have been isolated from *M. aeruginosa*. These include the microcystins, microginins (**32**), micropeptins (**33**), and aeruginosins (**34**)(Figure 14). The microginins (**32**) are linear peptides that act as amino-protease inhibitors, including leucine aminopeptidase, aminopeptidase M, and angiotensin-converting enzyme inhibitors (Ishida, 2000; Reshef, 2001). The micropeptins (**33**) contain a cyclic depsipeptide and have been found to act as a serine protease inhibitor as well as inhibitors of plasmin and thrombin (Ishida, 1995; Reshef, 2001). Lastly are the aeruginosins (**34**), a linear peptide, commonly found to inhibit trypsin and thrombin (Ishida, 1999; Murakami, 1995) and also show cytotoxicity against P388 murine leukemia cells (Ishida, 2002).



A: Micropeptin SD944 (**33**)



B: Microginin 478 (**32**)



C: Aeruginosin 98-B (**34**)

Figure 14: Examples of Toxins from *Microcystis aeruginosa*

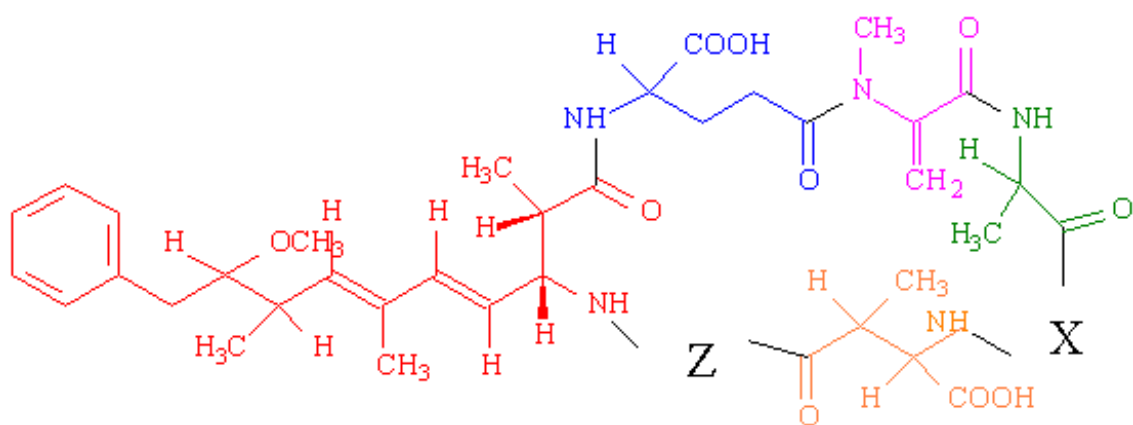
A) Micropeptin SD944 (**33**)

B) Microginin 478 (**32**)

C) Aeruginosin 98-B (**34**)

Of all the *M. aeruginosa* metabolites that are known, it is the microcystins that are the greatest threat to public health. Microcystins are also produced by other species of cyanobacteria, including *Microcystis viridis*, *Nostoc* sp., *Oscillatoria agardhii*, and *Anabaena flos-aquae* (Harada, 1988). However, of all the toxin producing species, the most predominant producer of microcystins is *M. aeruginosa*. From these particular species over 60 microcystin derivatives have been found to make up the group of microcystins. Among these, Microcystin LR (**35**) is the most abundant and has been found to have the greatest toxicity (Hyenstrand, 2001; Lawton, 2001).

These microcystin derivatives are cyclic heptapeptides containing a seven-membered peptide ring, composed of five non-protein amino acids and two protein amino acids. As seen in Figure 15, these heptapeptides are composed of γ -linked D-glutamic acid (D-Glu), D-alanine (D-Ala), β -linked D-erythro- β -methylaspartic acid (D-MeAsp), N-methyldehydroalanine (Mdha), a unique C₂₀ β -amino acid (Adda), and two variable L-amino acids. In most cases, variability in the structure is only seen at the protein amino acid positions, although other variations can occur (Matthiensen, 2000). Such variability leads to changes in the hydrophobicity and acidity of the specific compound. Those microcystins, which have tryptophan or phenylalanine as one of the variable amino acids, are generally more non-polar than those without (Lawton, 1995). Some specific examples of the variable amino acids can be found in Figures 15.



	X	Z
Microcystin LR	Leu	Arg
Microcystin RR	Arg	Arg
Microcystin YR	Try	Arg
Microcystin LF	Leu	Phe

Figure 15: General Structure of Microcystins; Variable protein L-amino acids at position X and Z

Microcystins are hepatotoxins that target the liver and show many destructive physiological effects, including distortion of the liver architecture, rearrangement of cellular organelles, and internal bleeding of the liver. (Codd, 1995; Falconer, 1988; McDermott, 1995). All of these physiological effects occur due to specific biochemical reactions that take place. Specifically, these toxins have been found to inhibit the serine/threonine protein phosphatases PP1 and PP2A (Bell, 2001). These protein phosphatases are crucial enzymes in tumor suppression and when inactivated by microcystins can cause the development of tumors (Lawton, 1995).

Human exposure to microcystins has been reported in several instances. The most serious occurrence took place in Caruaru, Brazil in 1996. When 60 patients died of acute liver failure after having undergone dialysis where microcystin contaminated the water that was used (Hummert, 1999). In addition to humans, microcystins have also caused the death of many farm animals (Hummert, 1999).

A number of methods for the detection of microcystins have been reported (Lawton, 2001). These include chemical detection based on LC/UV and biochemical methods using protein phosphatase assay or ELISA (enzyme-linked immunosorbant assay). All of these methods leave room for improvement based on their cross-reactivity and inability to quantify the amount of toxins present or provide an accurate profile of the toxins present. For instance, the ELISA test is based on the molecular recognition by certain antibodies, and the antibody will have different specificity towards each microcystin variant (Lawrence, 2001; Bouaicha, 1996). This causes the assay to inaccurately detect total microcystin content and leads to the possibility of false positives (Harada, 1988). The protein phosphatase assay functions as a measure of phosphatase

inhibition, but the assay may detect not only microcystins, but also unrelated compounds such as okadaic acid (another phosphatase inhibitor) and does not allow the differentiation between the microcystin variants (Harada, 1988; Lawrence, 2001). Of the methods under investigation, LC/UV has good potential for providing data on the toxin profile, but the method lacks sensitivity. As was previously mentioned, the current maximum allowable level of microcystins in drinking water is 0.1 µg/L. For this reason, a highly sensitive method must be developed to monitor and quantify these toxins. The purpose of this section of the thesis was to investigate and develop a new analytical method, based on LC/MS techniques for the detection of microcystins.

MICROCYSTIN EXPERIMENTAL

General

Sample concentration was carried out using 10 g/ 60 ml ENVI-18 Sep-pak columns (Supelco). HPLC/MS was performed using a Hewlett Packard 1100 coupled with a Waters Micromass mass spectrometer using a TSK-GEL Amide 80 column (2.0 x 100 mm) (Tosoh Biosep) or a Agilent Eclipse C₁₈ (2.0 x125 mm) column. Filtration was carried out using Whatman GF/A disks (30 cm diameter). Samples were sonicated using a Fisher Scientific FS60. All solvents were HPLC grade (Fisher). Concentration under reduced pressure was carried out using a Buchi rotoevaporator model R3000.

Microcystis aeruginosa Culture

All cultures were grown by Eve Wright using the following procedure. In a 1 L volumetric flask, 1 ml B₁₂ stock solution (Appendix 12), 1 ml biotin stock solution (Appendix 12), and 200 mg of thiamine HCl were combined. DI water was then added under analytical procedures. In a separate 1 L volumetric flask, 1 ml trace metal stock solution (Appendix 12), 3.15 g FeCl₃•6H₂O, and 4.36 g Na₂EDTA•2H₂O were combined. DI water was added under analytical procedures. Milli-Q water and the growth media solutions (total volume 1.5L) were added to each Fernbach flask. Flasks were autoclaved and allowed to cool for 24 hours, before inoculation with approximately 100 ml stock *Microcystis aeruginosa* cultures (100 mL). Cultures were incubated at room temperature for three weeks with daily agitation.

Extraction and Purification

Following growth, cultures were filtered and collected cells were stored in a freezer at -20°C for at least 24 hours. The filtrate was collected in 4 L amber glass bottles and stored at room temperature for further experimentation.

The cells collected on filter paper disks were extracted with 75% aqueous methanol (250 ml) sonicated, and left for an hour. The organic layer was decanted and the process was repeated two more times. The extracts were concentrated under reduced pressure.

In separate experiments the cells were extracted using 75% aqueous methanol/0.1% TFA as the extraction solvent. As a further comparison, another disk was extracted with 100% methanol/0.1% TFA. Each type of solvent extraction was carried out in triplicate and dried extracts were stored at -20°C for further experimentation. The organic material obtained in each extract was weighed and compared (Table 2).

Each crude extract was dissolved in 100% methanol (20 ml) and was filtered to remove any cell debris. The filtrate was concentrated under reduced pressure. This organic extract was fractionated using a Sep-pak cartridge activated with 3 column volumes of 100% methanol, then eluted with 3 column volumes of 20% aqueous methanol. The extract was taken up in 20% aqueous methanol (2 ml), briefly sonicated, and applied to the Sep-pak cartridge. The column was eluted with one column volume of each of the following solvent mixtures: 20%, 40%, 60%, 80%, and 100% methanol and, finally 100% hexane. Each gradient step and wash was collected separately and was concentrated under reduced pressure. The weight of each fraction was recorded.

	Trial 1			Trial 2			Trial 3		
	extract 1	extract 2	extract 3	extract 1	extract 2	extract 3	extract 1	extract 2	extract 3
75% MeOH	24.6 mg	13.4 mg	0.2 mg	27.9 mg	14.2 mg	1.4 mg	25.9 mg	13.3 mg	0.6 mg
75% MeOH/0.1% TFA	23.9 mg	14.1 mg	0.9 mg	24.3 mg	12.6 mg	0.8 mg	29.2 mg	14.7 mg	0.5 mg
100% MeOH/0.1% TFA	44 mg	7.2 mg	0.3 mg	38.5 mg	8.8 mg	0.2 mg	40.8 mg	7.6 mg	0.3 mg

Table 2: Comparison of Extraction Methods Based on Biomass Determination

The supernatant from filtered growth media was used as the source of “natural water” samples. This was used in the method development for analysis of raw water samples obtained from North Carolina lakes and reservoirs.

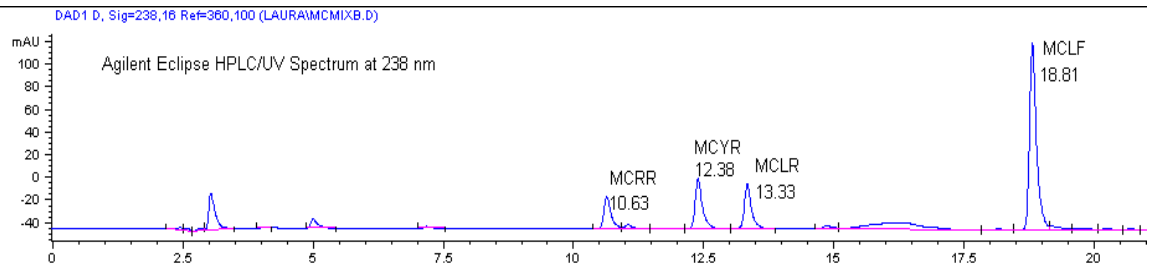
A Sep-pak cartridge was activated with 3 column volumes of 100% methanol, followed by the equilibration with 3 column volumes of 100% water. The “natural water” sample was passed through the Sep-pak cartridge at a flow rate of approximately 20 ml/min (1.5 L water/10g Sep-pak). Then the column was eluted with 20% and 100% methanol. Each fraction was collected separately, concentrated under reduced pressure, and stored at -20°C (the weights of each were recorded) This procedure was carried out three times in entirety to determine reproducibility.

HPLC/UV Method Development

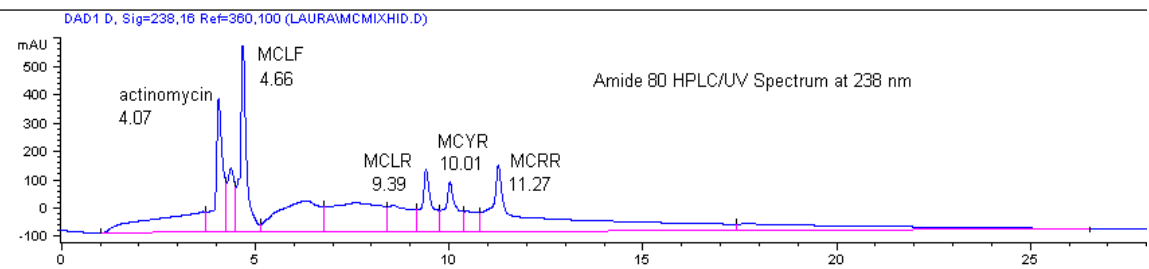
Various methods were carried out using four microcystin research samples (MCLR (35), MCRR (37), MCYR (36), MCLF (38)). Following experimentation, LC conditions used for all subsequent experiments are listed in Appendix 12. The traces shown in Figure 16 represent the HPLC chromatograms obtained from the use of the standard HILIC and reversed phase column methods. From these chromatograms, the UV spectra of the microcystins were obtained (Appendix 13).

Detection of Microcystins Using LC/MS

Both the extracted cell fractions and the natural water fractions were processed in the same manner. Dried fractions were re-dissolved in 50% aqueous acetonitrile (1 ml). For detection purposes, each fraction was run in duplicate using the HILIC conditions described in Appendix 12. The injection volumes for the cell extract fractions and the natural water fractions were 40 µl and 200 µl, respectively. Each fraction was run



A. Standard Trace of Microcystin Standards on Reversed Phase Column



B. Standard Trace of Microcystin Standards on HILIC Column

Figure 16: HPLC/UV Traces of Microcystin standards
 A) Standard Trace of Microcystin Standard on Reversed Phase Column
 B) Standard Trace of Microcystin Standards on HILIC Column

through the HPLC system and the compounds were monitored with both a diode array detector (DAD) and a mass spectrometer (MS). The conditions of the mass spectrometer can be found in Appendix A. Microcystin presence was determined based on their retention time, UV maximum, and $[M + H]^+$ values. Mass spectra of the microcystin standards can be seen in Appendix 14. A comparison between effectiveness of the various extraction techniques was carried out using these HPLC/UV/MS methods. A comparison of these methods can be found in Table 3.

Preparation of Quantification Standards

An aliquot (ca. 50 μg) of each microcystin standard was weighed out using a Cahn 28 Electrobalance, and the final weight of each was recorded. Four samples of the internal standard, actinomycin D (50 μg), were prepared as above. Each microcystin standard was placed into a separate vial and an actinomycin D samples was added to each. Methanol (200 μl) was added and the vial sonicated. Each disk was then removed and washed with MeOH (100 μl) into the corresponding vial, and the MeOH removed in vacuo. Serial dilutions of each of the four microcystin standards were carried out in the same manner. The final concentrations for each dilution can be found in Table 4.

Quantification

Using the LC/MS method previously developed for the Amide 80 column and the QuanLynx program, calibration curves were created. Quantification parameters for each of the microcystin standards were based on peak area as compared to the internal standard, actinomycin. Each standard peak was selected based on retention time ± 0.2 minutes, and based on these, calibration curves were produced using a linear polynomial,

MCLR Presence		
MeOH Elution	MS Detection	UV Detection
20%	N	N
40%	N	N
60%	Y	Y
80%	N	N
100%	N	N
Hexane	N	N

A: Extraction with 75% aqueous MeOH/0.1% TFA

MCLR Presence		
MeOH Elution	MS Detection	UV Detection
20%	N	N
40%	N	N
60%	Y	N
80%	N	N
100%	N	N
Hexane	N	N

B: Extraction with 75% aqueous MeOH

Table 3: Comparison of Extractions With and Without TFA through Mass Spectrometer and Ultraviolet Detection of MCLR
 A) Extraction with 75% aqueous MeOH/0.1% TFA
 B) Extraction with 75% aqueous MeOH

Standard	Stock Solution Concentration	Dilution 1 Concentration	Dilution 2 Concentration	Dilution 3 Concentration
MCLR	102.5 µg/ml	25.6 µg/ml	6.4 µg/ml	1.6 µg/ml
MCRR	117.5 µg/ml	29.5 µg/ml	7.8 µg/ml	1.9 µg/ml
MCYR	360.0 µg/ml	120.0 µg/ml	40.0 µg/ml	13.0 µg/ml
MCLF	55.0 µg/ml	27.5 µg/ml	13.8 µg/ml	6.9 µg/ml

Table 4: Quantification Standard Concentrations for Each Microcystin Standard

excluding the point of origin, and fit weighting the line to $1/X$. For each of the microcystin standards, the four serial dilutions were run in sequence and their MS response was monitored and incorporated into the QuanLynx program for analysis. Based on the pre-programmed conditions just mentioned, the response of each of the dilutions was plotted versus the concentration ($\mu\text{g/ml}$), Figure 17. Each standard was run in duplicate. Each duplicate calibration curve was averaged to give the final curves for each type of calibration.

Following the development of MS calibration curves, UV calibration curves were produced. The same MCLR (35) serial dilution standards were used and the UV peak area response was monitored. The injected amount (μg) was then plotted versus the UV response (Figure 18).

A. Mass Spectrometer Response vs. Concentration

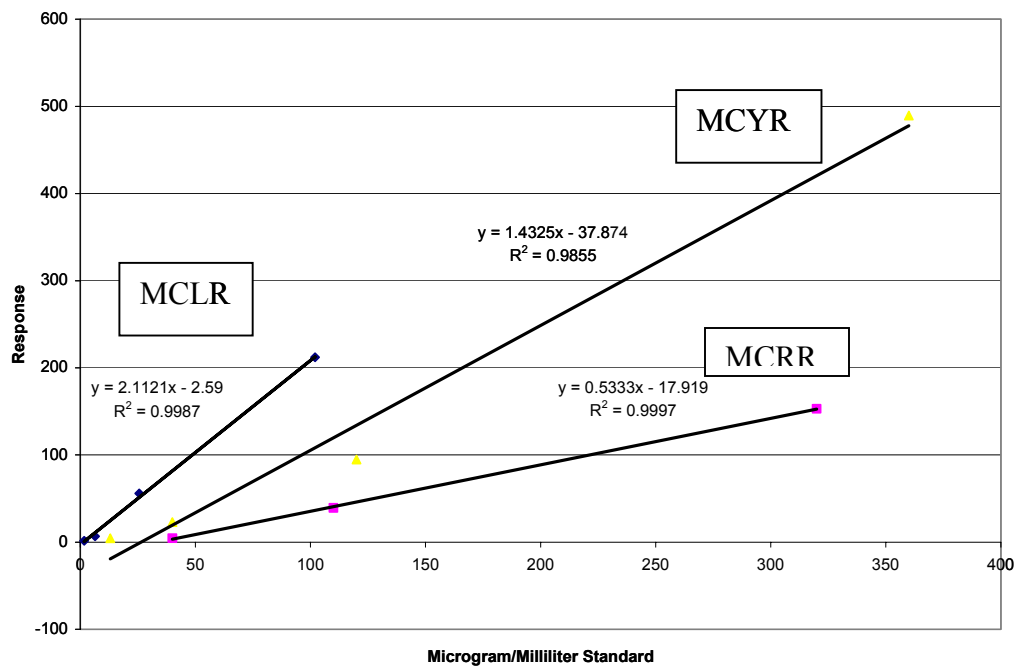


Figure 17: Standard Calibration Curves of Three Microcystin Derivatives Based on Mass Spectrometer Response ($\mu\text{g/ml}$ of injected sample)

UV Response vs. Mass Injected

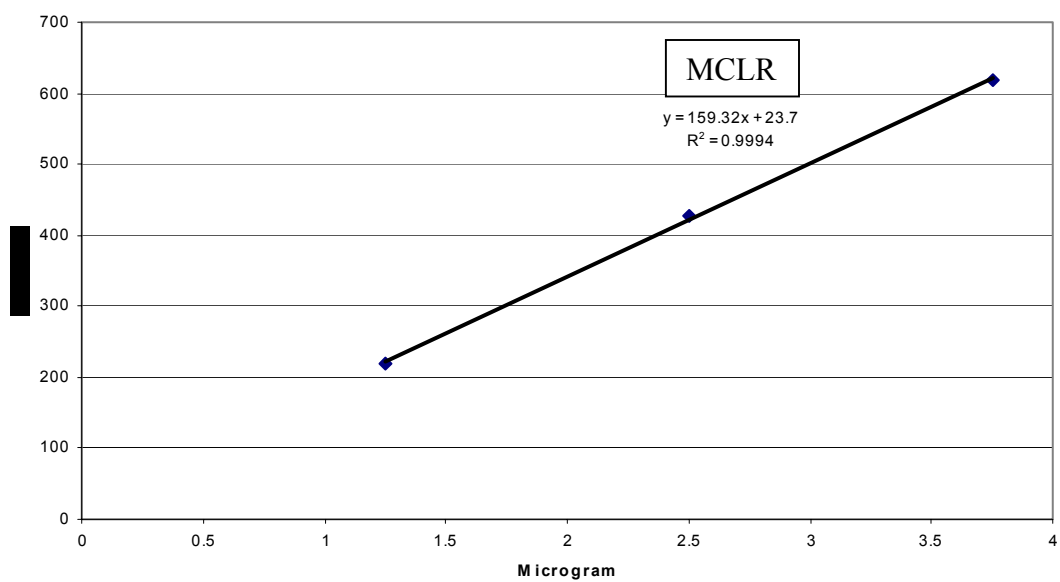


Figure 18: Calibration Curve of Microcystin LR based on UV Response (μg injected)

MICROCYSTIN RESULTS

Efficiency of Solvent Extractions

Three different solvent extraction methods were compared to determine the most efficient for recovery of microcystins with the least dissolved organic matter. Two extraction solvents were considered: 100% methanol and 75% aqueous methanol. The pure organic extraction was found to extract approximately 17 % more total biomass on average. However, TLC comparisons of the two extracts indicated considerably more chlorophyll was present in the organic extract. After comparing these results, the aqueous organic solvent was selected to reduce the interference of the chlorophyll.

Further improvement in microcystin extraction was achieved by adding 0.1% TFA (trifluoroacetic acid). This was determined by LC/MS analysis of the fractions obtained following separation on a Sep-pak cartridge. Each fraction was injected in the same concentration and was run in duplicate to ensure accurate detection (Table 3). Based on these results it can be deduced that the 75% aqueous methanol/0.1% TFA extract had a greater amount of MCLR (**35**) present, due to the detection of MCLR (**35**) by UV (a less sensitive measuring technique) in the TFA extract.

Optimum extraction repetition for complete toxin extraction was determined for each solvent extraction and compared (Table 2). Once again based on these experiments it was found that two extractions were sufficient, since only 1% additional biomass was obtained in the third extraction, regardless of the solvent used. From these experiments the optimum procedure was determined to be a double extraction of the cells using 75% aqueous MeOH/0.1% TFA.

Efficiency of Extract Fractionation

The efficiency of the initial Sep-pak clean-up step of the crude extract was tested using LC/MS analysis. The crude extract was eluted with: 20%, 40%, 60%, 80%, 100%: methanol and 100% hexane, and each fraction was monitored by LC/MS. MCLR (**35**) was only found in the 60% aqueous methanol fraction (Table 3).

Further experimentation of the clean-up step for raw water samples was carried out by passing the raw water samples through a 10g/60ml Sep-pak cartridge. After passing 1.5 L of water through the column, material began to diffuse slightly down the column. Based on this, the column was changed every 1.5 L to ensure that the organics were retained on the column. The column was then washed with 20% aqueous methanol followed by elution with 100% methanol. The aqueous organic fraction contained about 26% of unwanted material (by weight), with no microcystins present by LC/MS analysis. In contrast the organic fraction contained both MCLR (**35**) and MCRR (**37**).

HPLC Method Development

Two different chromatography systems were examined: the reversed phase method using a C₁₈ column, and another based on hydrophilic liquid interaction chromatography (HILIC). Of most importance was baseline separation of the microcystins to permit accurate quantification of microcystins present in collected fractions. Other features such a run duration, sharpness of peaks, and absence of compounds in the solvent front were also important considerations.

Reversed phase chromatography was performed using an Agilent Eclipse C₁₈ column, and while a few of the methods allowed some separation, only one method showed complete resolution and sharpness of peaks (Figure 16).

In an alternate approach (HILIC) an Amide 80 column was used, which is typically used for peptides such as the microcystins. Although all microcystins were resolved using a simple gradient, a more complex procedure was required to clean the column. Specifically this method allowed baseline separation of MCLR (**35**) and MCYR (**36**), which was not found in previously developed methods. Another feature of this HILIC approach was the juxtaposition of two different separation methods, namely reversed phase and HILIC, to reduce the effect of interfering peaks in the final LC/MS analysis step. This was indeed found to be the case and the HILIC method had the added advantage of good separation over a slightly shorter run time. The only drawback to the use of the Amide 80 column is the rapid elution of the more non-polar microcystins, such as MCLF (**38**).

Comparison between LC/UV and LC/MS Detection

In some cases UV detection can be seen as a qualitative feature, since the absorbance of a compound is mainly based on the functionality of the molecule and is dependent on the wavelength the absorbance is monitored at, while MS detection is a quantitative measure. This is due to the fact that peak height/area is directly related to the amount of compound present.

Due to this, from this analysis the limit of detection (LOD) for UV detection was found to be 3.6 $\mu\text{g/L}$, while for MS detection the LOD was 0.08 $\mu\text{g/L}$, based on initial sample concentration. These values are very important when determining the most efficient method to monitor drinking water supplies. Due to current standards in drinking water, 0.1 $\mu\text{g/L}$, UV detection would not be able to detect these low concentrations of

toxins. For this reason MS detection is more reliable method for monitoring microcystin levels.

Calibration Curves

With the exception of MCLF (**38**), calibration curves were attainable for the microcystin standards. The amount of MCLF (**38**) standard that was available was not sufficient to acquire accurate readings with either UV or MS detection. The most concentrated **38** sample (55 μ g/ml) caused a small MS response, but upon making even slight dilutions (27.5 μ g/ml) the detection by MS was no longer possible. While MCLF (**38**) did not give accurate readings, the other three microcystin standards gave good readings. These three standards were run in duplicate to ensure repeatability. From the testing, the calibration curves were within acceptable limits of error based on their R values and consistency between duplicate curves was present. From the MS calibration curves it was determined that there was a linear response and was within the limits of error. The MS calibration curve was compared to UV detection. The same MCLR dilutions were used and produced a linear curve comparable to that from MS detection.

Both MS and UV calibration curves for **35** are linear, but the UV curve has a slightly higher R value. Of further comparison is the positive y-intercept in the case of the UV calibration curve, likely due to background absorbance. Another difference is the increased slope of the UV calibration curve, 159.32, while the MS slope was 105.79. This could possibly be due to amplification of absorbance when more compound is present. In other words as more of the same compound is present the ability of excitation becomes increasingly easier, resulting in amplification of absorbance.

MICROCYSTIN DISCUSSION

As the frequency of blue-green algal blooms in drinking water supplies becomes more frequent, the need to efficiently and accurately measure the presence of algal toxins in the waters is rising. While the presence of blue-green algae toxins are known, they are considered unregulated known contaminants, according to the Environmental Protection Agency. At this point, the problem has been established, but specific monitoring techniques and regulations have not been enacted. Currently in the United States there are no regulations to address this problem, but recently, steps have been taken by the North Carolina Department of Health to monitor the presence of these toxins, specifically microcystins.

Due to the possible health risks associated with blue green algal toxins, there is a need for an accurate detection and quantification of these toxins. To date, various methods have been reported for the detection of microcystins, but each has several crucial drawbacks. The ELISA test has the promise of sensitivity and of rapid results, but the selectivity of the analysis is unknown, and could be subject to interferences from unrelated compounds. Analytical methods such as LC/UV have been explored but the drawback here is the sensitivity and the lack of absolute quantification due to absorbance variability. Thus, while these methods provide some useful data, neither allows absolute detection and quantification of these hepatotoxins. For these reasons a more definitive analytical method is required.

Within this study, the detection and quantification of microcystins at sub-allowable levels has been successfully applied to laboratory and North Carolina drinking

water supply samples through the use of LC/MS. This approach permits the identification of individual microcystin derivatives within a complex mixture. In addition to the accurate monitoring of these toxins, the extraction and concentration of both water and cell samples has been developed to quickly and effectively purify and concentrate the microcystins present. The detection sensitivity of this method for the analysis of microcystins is 0.08 $\mu\text{g/L}$, which is below the current allowable levels for microcystins in drinking water currently in effect in many countries.

The development of accurate calibration curves using LC/MS was necessary to allow quantification of natural samples. Accurate calibration curves were developed for the more common microcystin derivatives: MCLR (35), MCRR (37), and MCYR (36) during this study. Each of these curves is accurate between the range of 2.3-400 $\mu\text{g/ml}$ permitting the determination of toxin levels within this range. The efficiency of the extraction and concentration methods was optimized in order to remove the majority of the unwanted compounds and concentrate the microcystins present within the limits of accurate quantification. In the case of natural water samples, the clean-up method was found to extract microcystins from the water sample and concentrate to sample by at least 100-fold. Through the use of the detection and quantification methods developed within this work, the presence of microcystins and concentration determinations were able to accurately be determined. Within this study, virtually unambiguous detection of microcystins has been achieved allowing affective monitoring of drinking water supplies.

From the results obtained in this work, future research topics have been identified. While the methods here allow for the easy detection and quantification of the most common microcystins, 57 other known minor variants do exist. Currently, only six of the

microcystin variants are commercially available, and even then the cost of these compounds is prohibitive (\$250/ μg). The availability of microcystin standards would facilitate quantification of all the known variants, and frequent calibration checks of the equipment and analytical method. Consequently, the development of simple isolation methods for the major and minor microcystins is essential.

Another area of interest evolves from the collection of samples from the field. Based on the amount of water that needs to be collected (approximately 1L) for accurate analysis, it would be helpful to develop a method that permits concentration of water samples in the field. Such a method would require the development of solid phase extraction (SPE) cartridges, through which large volumes of water could be passed. This would also require the application of a pressure system, to rapidly push the water through the cartridge. The benefit of this would be that instead of leaving collection sites with liters of water, only several convenient cartridges would be required.

It may also be possible to shorten the length of each analytical run. An approach to reduce the length of the LC/MS method would be the development of an isocratic LC system. Such a method was not found in the present studies that sufficiently separate the standards for quantification, there are still many chromatography variables that can be examined. There is also interest in the development of detection and quantification methods by MS alone, which would save time by circumventing the LC steps. While this would result in a loss of checks and balances between the mass spectrometer scan and the retention time of the standards, it would greatly decrease the amount of time to run each sample. While a method of this type would not be able to give accurate confirmation of the microcystins present, but this quick method would allow a way to determine which

samples need further testing by LC/MS. All of these techniques and procedures would further the efficiency of the methods found within these studies and enable easier detection of these toxins.

MICROCYSTIN CONCLUSIONS

Based on these results, a rapid and accurate method has been established for the detection of microcystins using LC/MS techniques. The limit of detection for this method was found to be 0.08 µg/L, which is more sensitive than the known allowable levels in drinking water supplies. Further emphasis is found in the development of calibration curves for the most common microcystins enabling the determination of toxin concentration in water supplies. All of the procedures have lead to the unambiguous determination of the amount of microcystins present and differentiation of microcystin variants.

Literature Cited

- Bangera, M. G.; Thomashow, L. S. *Journal of Bacteriology*. **1999**, 181, 3155-3163.
- Bauer, W. D.; Robinson, J. B. *Current Opinion in Biotechnology*. **2002**, 13, 234-237.
- Bell, S.G.; Codd, G.A. Detection, Analysis and Risk Assessment of Cyanobacterial Toxins. **2001**, 109-122.
- Bouaicha, N.; Rivasseau, C.; Hennion, M.; Sandra, P. *Journal of Chromatography B*. **1996**, 685, 53-57.
- Brelles-Marino, G.; Bedmar, E. J. *Journal of Biotechnology*. **2001**, 91, 197-209.
- Brodersen, D. E.; Clemons, W. M.; Carter, A. P.; Morgan-Warren, R. J.; Wimberly, B. T.; Ramakrishnan, V. *Cell*. **2000**, 103, 1143-1154.
- Cho, M. K.; Sung, M.; Kim, D. S.; Park, H. K.; Jew, S. S.; Kim, S. G. *International Immunopharmacology*. **2003**, 520, 1-9.
- Codd, G.A. *Water Science Technology*. **1995**, 32, 149-156.
- Crews, P.; Rodriguez, J.; Jaspars, M. Organic Structure Analysis. **1998**, Oxford University Press, Inc.
- DeLisa, M. P.; Bentley, W. E. *Microbial Cell Factories*. **2002**, 1, 1-25.
- Dewick, P. M. Medicinal natural products: a biosynthetic approach.. **2002**, Wiley, 2nd edition.
- Donabedian, H. *Journal of Infection*. **2002**, 11, 1-8.
- Eliasson, C.; Kamal-Eldin, A.; Andersson, R.; Amna, P. *Journal of Chromatography A*. **2003**, 1012, 151-159.
- El-Sayed, A. K.; Hothersall, J., Thomas, C. M. Quorum-sensing-dependent regulation of iosynthesis of the polyketide antibiotic mupirocin in *Pseudomonas fluorescens*. **2001**, 2127-2139.
- Fakhouri, W.; Walker, F.; Vogler, B.; Armbruster, W.; Buchenauer, H. *Phytochemistry*. **2001**, 58, 1297-1303.
- Falconer, I. R.; Smith, J. V. *Journal of Toxicology and Environmental Health*. **1988**, 24, 291-305.

- Fogg, G. E.; Stewart, W.; Fay, P.; Walsby, A. *The Blue-Green Algae*. **1999**, pps. 11, 97, 100, 133, 136, 257, 263-264.
- Harada, K.; Matsuura, K.; Suzuki, M. *Journal of Chromatography*. **1988**, 448, 275-283.
- Holden, M.T.G.; Chhabra, S.; de Nys, R.; Stead, P.; Bainton, N. J.; Hill, P. J.; Manefield, M.; Kumar, N.; Labatte, M.; England, D.; Rice, S.; Givskov, M.; Salmond, G. P.C.; Stewart, G.; Bycroft, B. W.; Kjelleberg, S.; Williams, P. *Molecular Microbiology*. **1999**, 33, 1254-1266.
- Hummert, C.; Reichelt, M.; Legrand, C.; Graneli, E.; Luckas, B. *Chromatographia*. **1999**, 50, 173-180.
- Hyenstrand, P.; Metcalf, J.S.; Beattie, K.A.; Codd, G.A. *Toxicon*. **2001**, 39, 589-594.
- Ishida, K.; Kato, T.; Murakami, M.; Watanabe, M.; Watanabe, M. *Tetrahedron*. **2000**, 56, 8643-8656.
- Ishida, K.; Matsuda, H.; Okita, Y.; Murakami, M. *Tetrahedron*. **2002**, 58, 7645-7652.
- Ishida, K.; Murakami, M.; Matsuda, H.; Yamaguchi, K. *Tetrahedron Letters*. **1995**, 36, 3535-3538.
- Ishida, K.; Matsuda, H.; Okino, T.; Murakami, M. *Tetrahedron*. **1999**, 55, 10971-10988.
- Jew, S.; Yoo, C.; Lim, D.; Kim, H.; Mook-Jung, I.; Jung, M.; Choi, H.; Jung, Y.; Kim, H.; Park, H.. *Bioorganic & Medicinal Chemistry Letters*. **2000**, 10, 119-121.
- Klare, I.; Konstabel, C.; Badstubner, W.; Witte, W. *International Journal of Food Microbiology*. **2003**, 2779-2800.
- Lawrence, J. F.; Menard, C. *Journal of Chromatography A*. **2001**, 922, 111-117.
- Lawton, L.; Edwards, C. *Journal of Chromatography A*. **2001**, 912, 191-209.
- Lawton, L. A.; Edwards, C.; Beattie, K. A.; Pleasance, S.; Dear, G. J.; Codd, G. *Tetrahedron Letters*. **1995**, 36, 3010-3016.
- Lebuhn, M.; Heulin, T.; Hartmann, A. *FEMS Microbiology Letters*. **1997**, 22, 325-334.
- Li, H.; Matsunaga, S.; Fusetani, N. *Comparative Biochemistry and Physiology Part B: Biochemistry and Molecular Biology*. **1994**, 107, 261-264.
- Loh, J.; Pierson, E. A.; Pierson, L. S.III; Stacey, G.; Chatterjee, A. *Current Opinion in Plant Biology*. **2002**, 5, 1-6.

- Malik, V.S. *Trends in Biochemical Sciences*. **1980**, 5, 68-72.
- Mantle, P. G.; DeLangen, M.; Teo, V. *The Journal of Antibiotics*. **2001**, 54, 166-174.
- Matthiensen, A.; Beattie, K. A.; Yunes, J. S.; Kaya, K.; Codd, G. A. *Phytochemistry*. **2000**, 55,383-387.
- McDermott, C.M.; Feola, R.; Plude, J. *Toxicon*. **1995**, 33, 1433-1442.
- Mehto, P.; Ankelo, M.; Hinkkanen, A.; Mikhailov, A.; Eriksson, J.E.; Spoof, L.; Meriluoto, J. *Toxicon*. **2001**, 39, 831-836.
- Meriluoto, J. A.O.; Eriksson, J. E. *Journal of Chromatography*. **1988**, 438, 93-99.
- Mossialos, D.; Meyer, J.; Budzikiewicz, H.; Wolff, U.; Koedam, N.; Baysse, C.; Anjaiah, V.; Cornelis, P. *Applied and Environmental Microbiology*. **2000**, 66, 487-492.
- Murakami, M.; Ishida, K.; Okino, T.; Okita, Y.; Matsuda, H.; Yamaguchi, K. *Tetrahedron Letters*. **1995**, 36, 2785-2788.
- Ohtake, A.; Shirai, M.; Aida, T., Aida; M., Naoyoshi, A.; Harada, K.; Matsuura, K.; Suzuki, M.; Nakano, M.; *Applied and Environmental Microbiology*. **1989**, 55, 3202-3207.
- Ongena, M.; Jacques, P.; Thonart, P.; Grove, I.; Fernandez, D.; Schafer, M.; Budzikiewicz, H. *Tetrahedron Letters*. **2001**, 42, 5849-5851.
- Osman, S. F.; Fett, W. F.; Irwin, P.; Cescutti, P.; Brouillette, J. N.; O'Conner, J. V. *Carbohydrate Research*. **1997**, 300, 323-327.
- Pfeifer, B. A.; Khosla, C. *Microbiology and Molecular Biology Reviews*. **2001**, 65, 106-118.
- Philson, S. B.; Llinas, M. *The Journal of Biological Chemistry*. **1982**, 257, 8081-8085.
- Reshef, V.; Carmeli, S. *Tetrahedron*. **2001**, 57, 2885-2894.
- Rivasseau, C.; Martins, S.; Hennion, M.. *Journal of Chromatography*. **1998**, 799, 155-169.
- Schauder, S.; Bassler, B. L. *Genes & Development*. **2001**, 15, 1468-1480.
- Seed, J.; Seed, T. M.; Sechelski, J. *Comparative Biochemistry and Physiology Part C: Comparative Pharmacology*. **1978**, 60, 175-185.
- Simpson, T. J. *Chemistry & Industry*. **1995**, 407-411.

Whitehead, N. A.; Barnard, A. M. L.; Slater, H.; Simpson, N. J.L.; Salmond, G. P. C. *FEMS Microbiology*. **2001**, 25, 365-404.

Williams, P.; Camara, M.; Hardman, A.; Swift, S.; Milton, D.; Hope, V. J.; Winzer, K.; Middleton, B.; Pritchard, D. I.; Bycroft, B. W. *Phil. Trans. R. Soc. Lond. B*. **2000**, 355, 667-680.

Withers, H.; Swift, S.; Williams, P. *Current Opinion in Microbiology*. **2001**, 4, 186-193.

Wolf- Watz, H.; Miller, V. L. *Current Opinion in Microbiology*. **2003**, 6, 3-6.

Wong, J. *Current Care Update for OB/GYNs*. **2003**, 10, 124-126.

<http://www.epa.gov> (EPA), **2003**

<http://epa.gov/safewater> (SDWA), **2003**

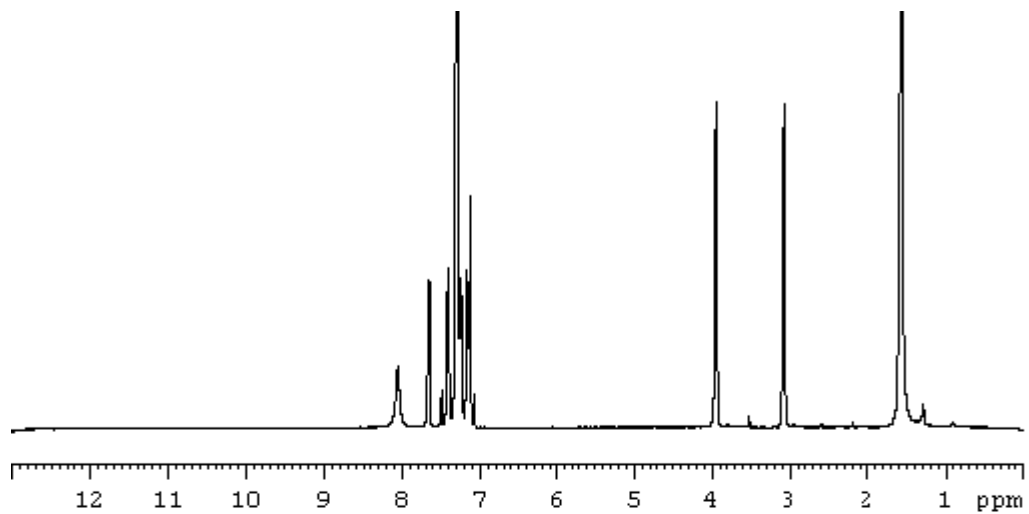
Appendix 1: Composition of Vanillin/H₂SO₄ TLC Spray

60 g vanillin

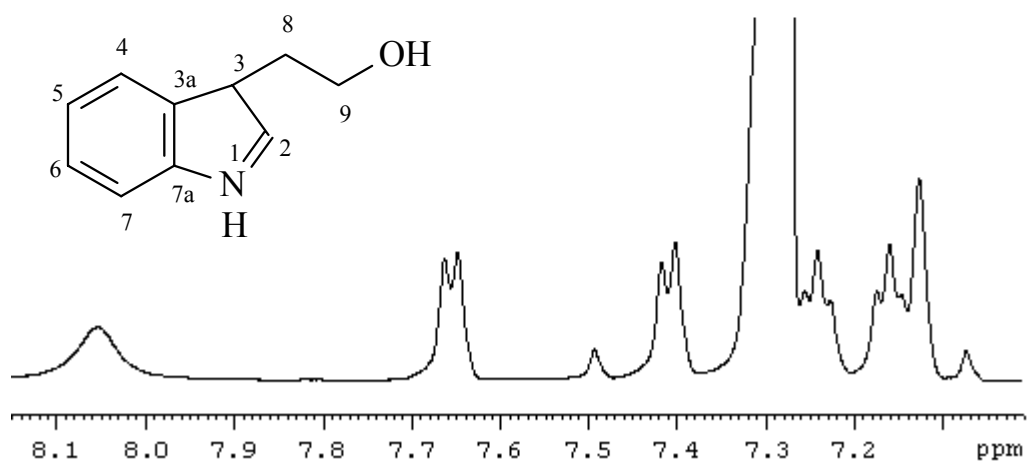
1 L 95% ethanol

10 ml sulfuric acid

Appendix 2: Proton NMR Spectra of Tryptophol (22)

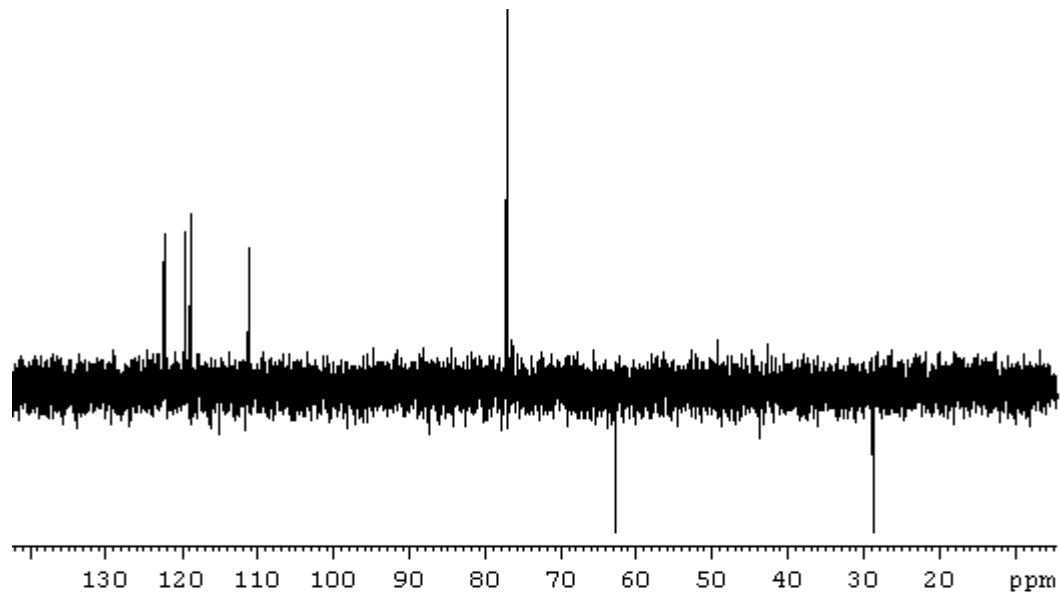


A: Proton NMR in Chloroform

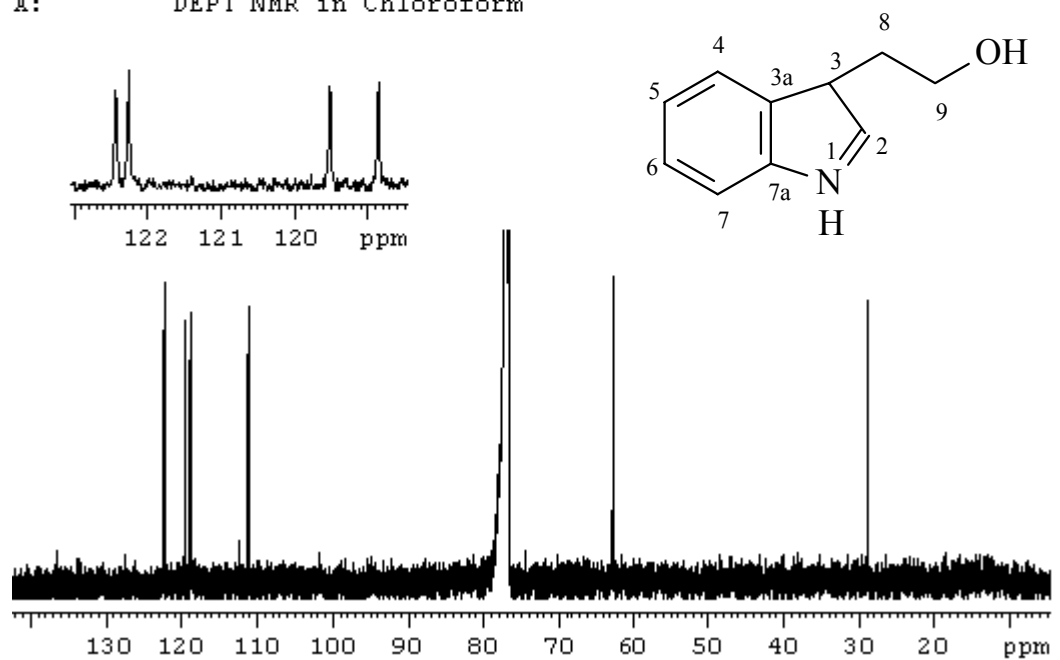


B: Expanded Region of Proton NMR in Chloroform

Appendix 3: Carbon and DEPT NMR Spectra of Tryptophol (**22**)

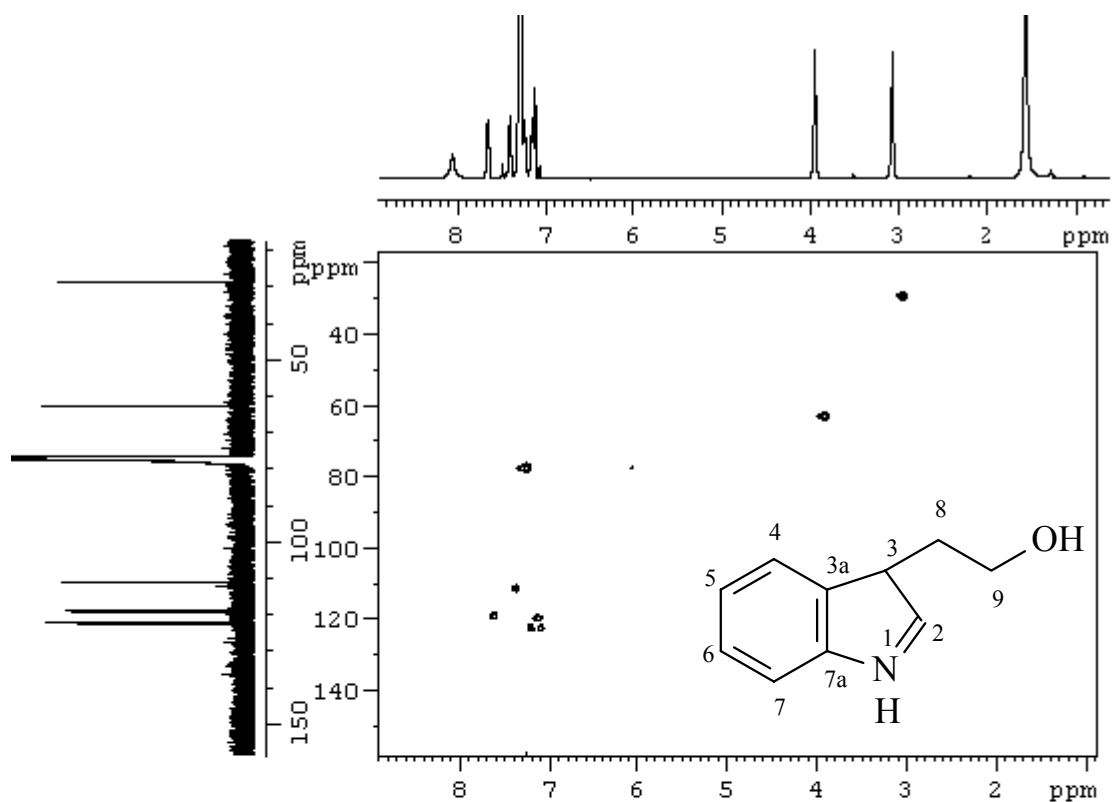


A: DEPT NMR in Chloroform

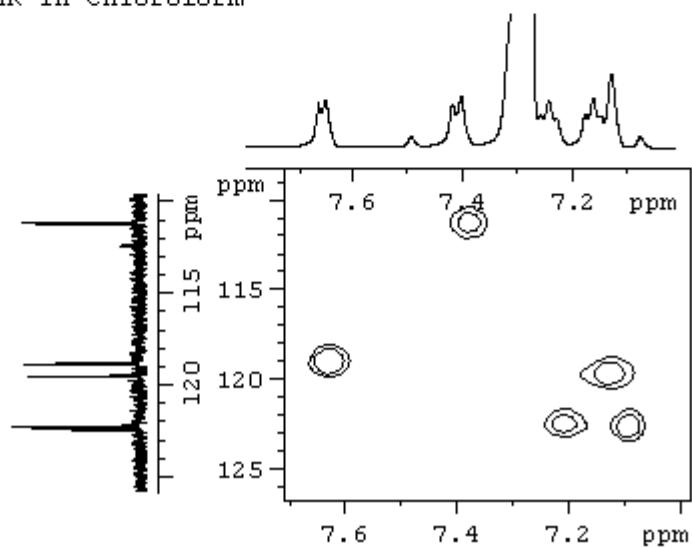


B: Carbon NMR in Chloroform

Appendix 4: HMQC Spectra of Tryptophol (22)

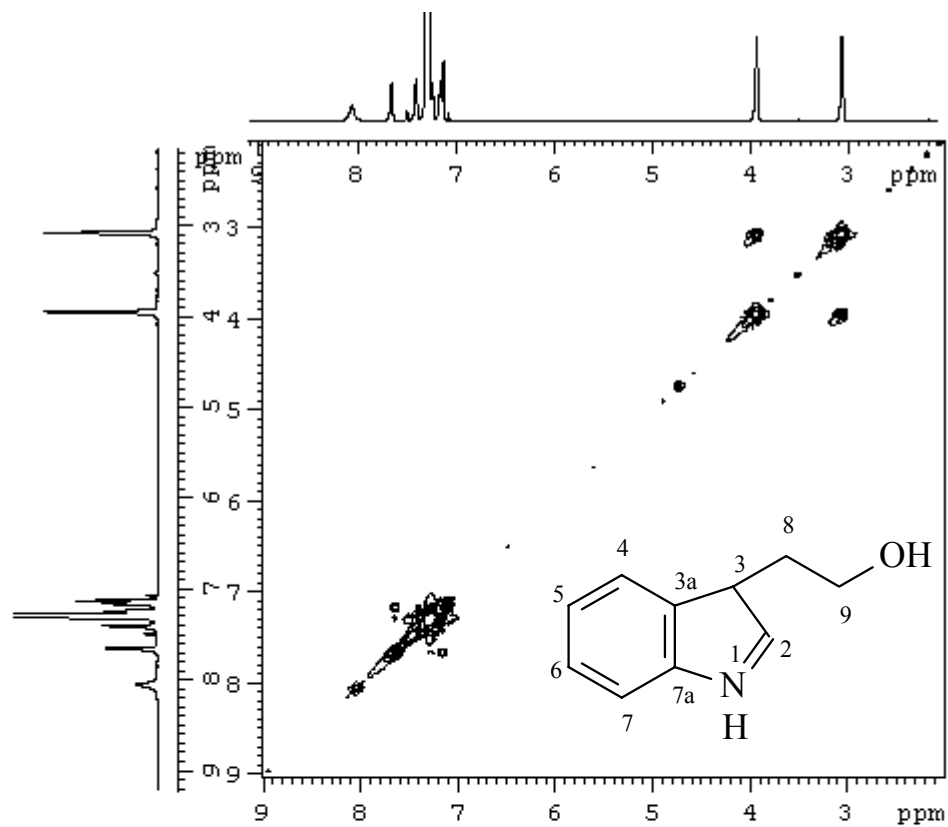


A: HMQC NMR in Chloroform

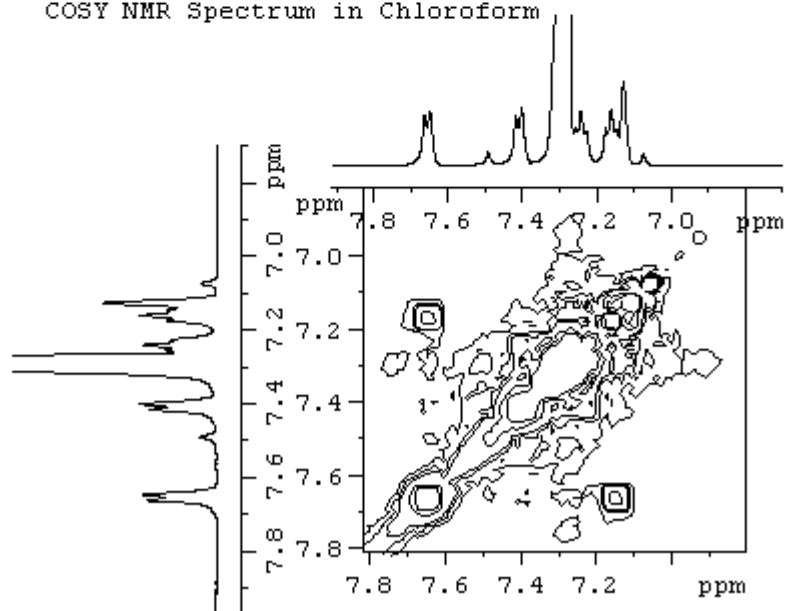


B: Expanded HMQC NMR in Chloroform

Appendix 5: COSY NMR Spectra of Tryptophol (22)

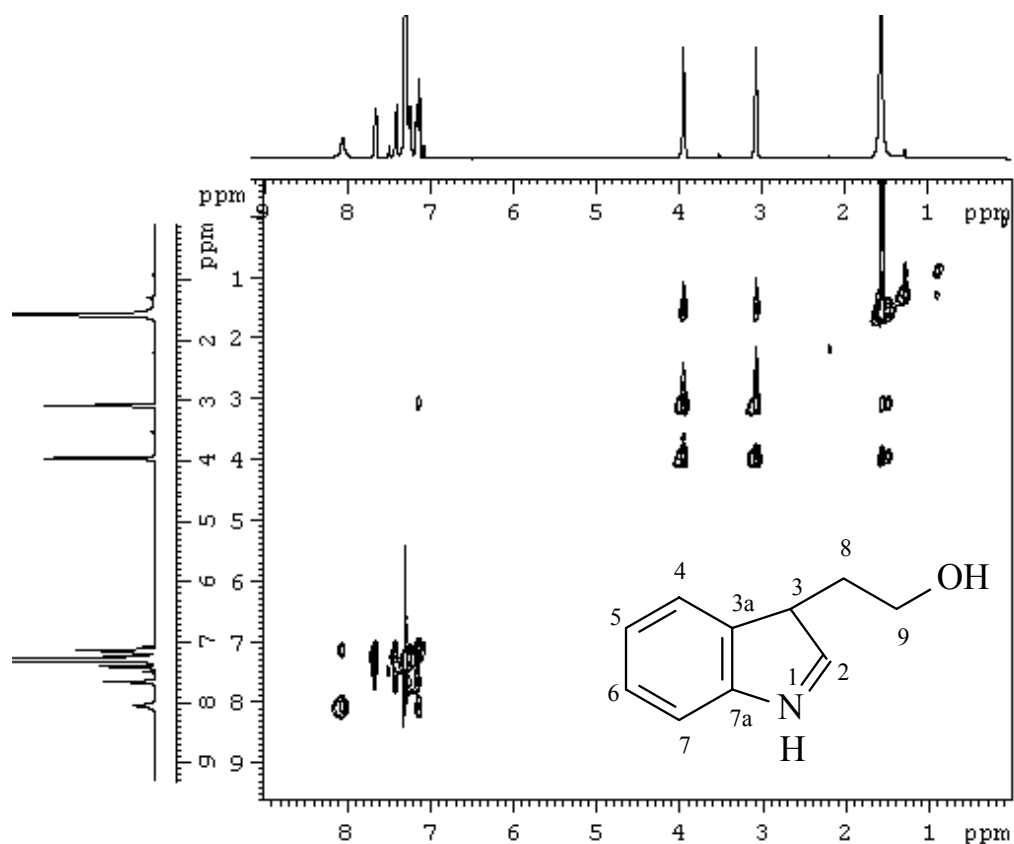


A: COSY NMR Spectrum in Chloroform

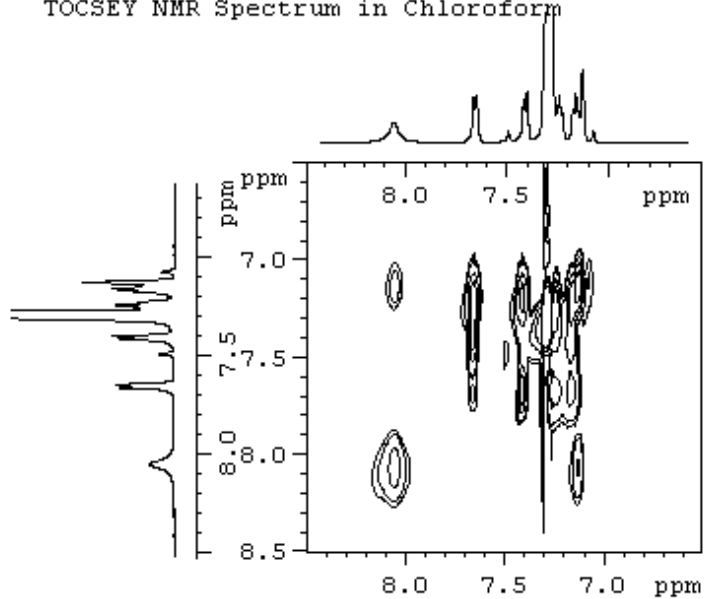


B: Expanded Region of COSY NMR Spectrum in Chloroform

Appendix 6: TOCSY NMR Spectra of Tryptophol (22)



A: TOCSY NMR Spectrum in Chloroform



B: Expanded Region of TOCSY NMR Spectrum in Chloroform

Appendix 7: Mass Spectrometer Conditions

ES Source:

Voltages:

Capillary (kV)	3.5
Cone (V)	25
Extractor (V)	5
RF lens (V)	0.5

Temperatures:

Source	125
Desolvation	350

Gas flow:

Desolvation	350
Cone	50

Analyser:

Analyser:

LM Resolution	15
HM Resolution	15
Ion Energy	0.5
Multiplier	650

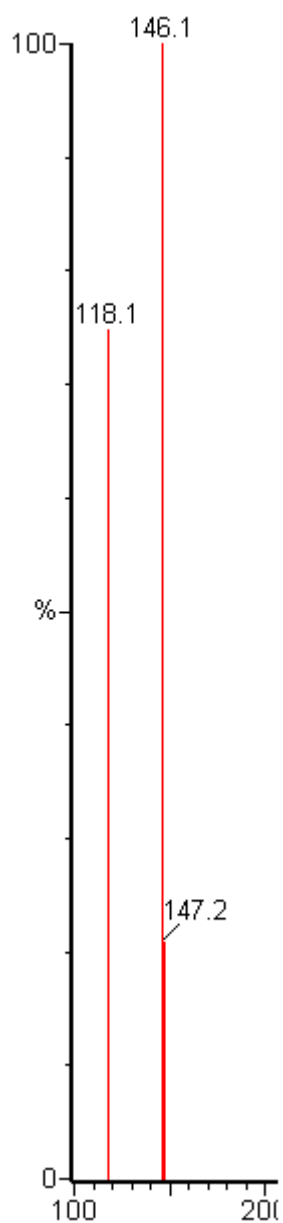
Syringe:

Pump flow	10 microliter/min
-----------	-------------------

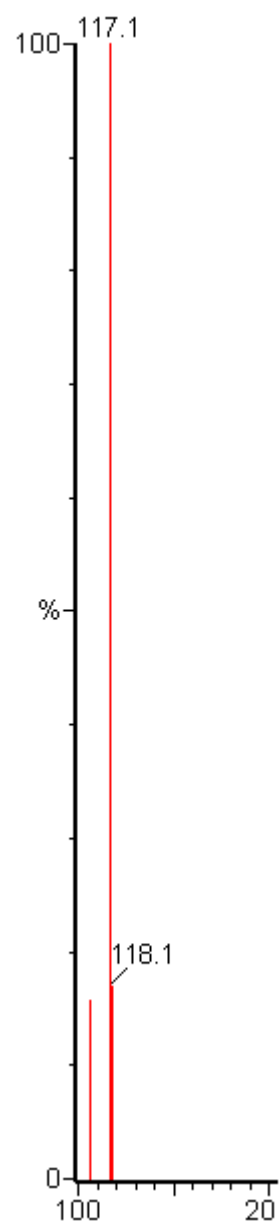
Mass Scan:

<u>Voltage</u>	<u>Mass Range</u>	<u>ES Mode</u>
25	100-1200	ES+/ES-
50	100-1200	ES+/ES-
75	100-1200	ES+/ES-
100	100-1200	ES+/ES-
125	100-1200	ES+/ES-

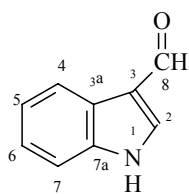
Appendix 8: Mass Spectra of indole-3-aldehyde (**23**) at 25 V and 75 V



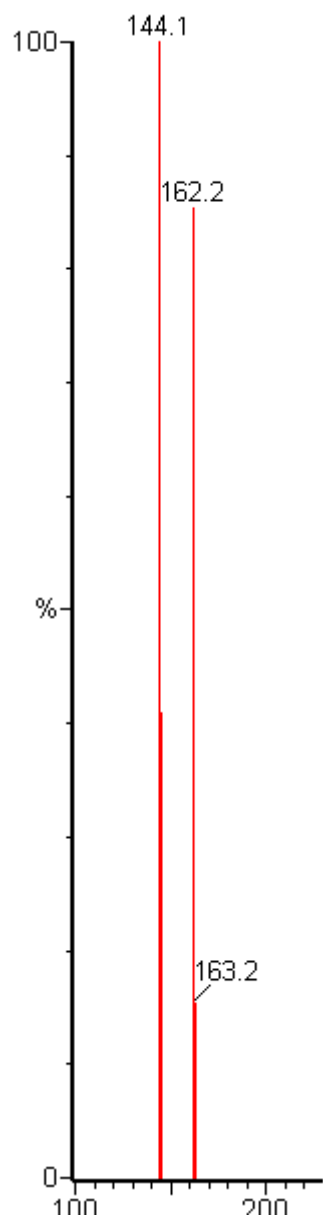
A: Mass Spectrum at 25 V



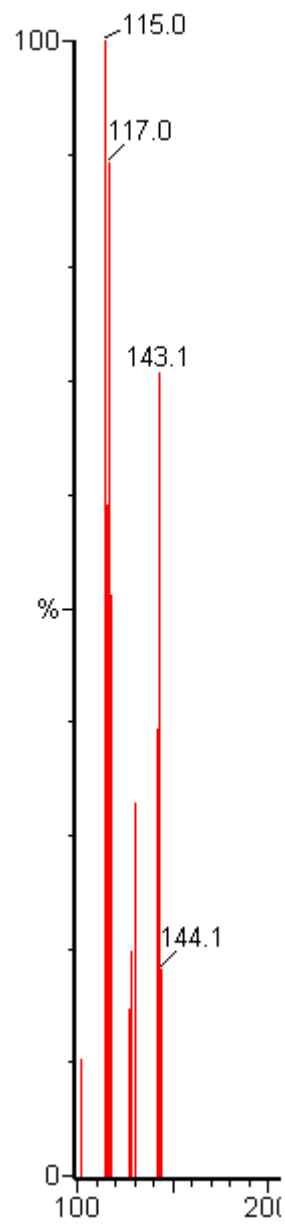
B: Mass Spectrum at 75 V



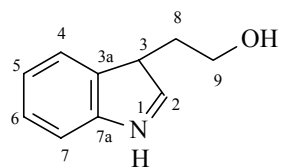
Appendix 9: Mass Spectra of Tryptophol (**22**) at 25 V and 75 V



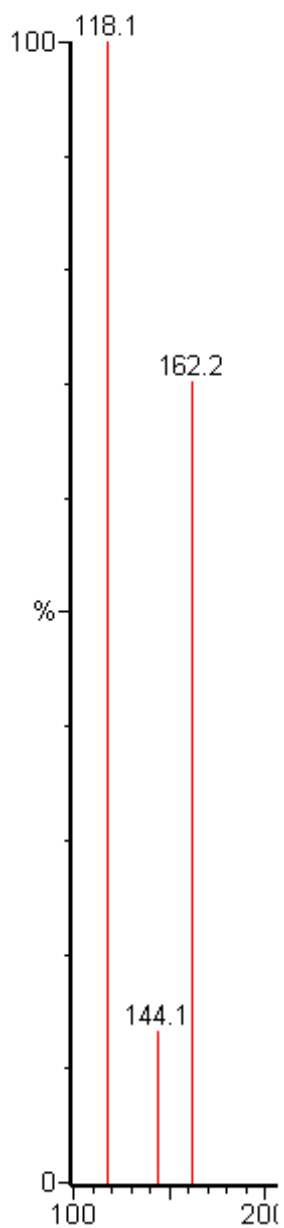
A: Mass Spectrum at 25 V



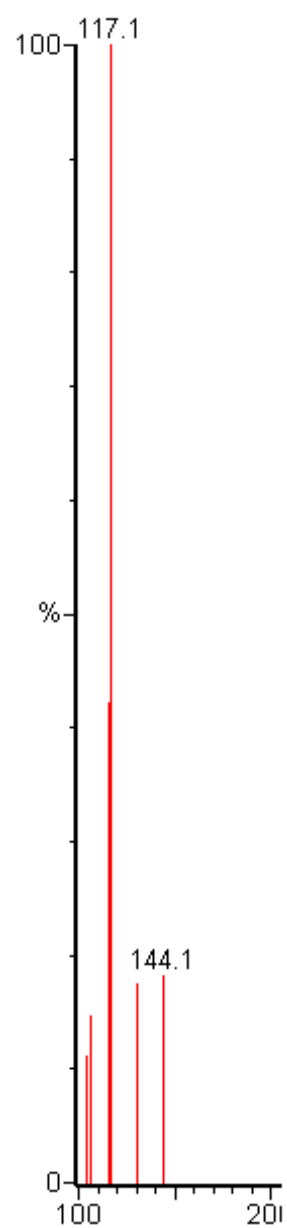
B: Mass Spectrum at 75 V



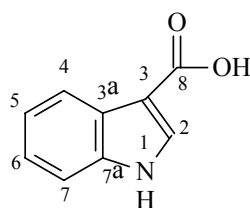
Appendix 10: Mass Spectra of indole-3-carboxylic acid (**24**) at 25 V and 75 V



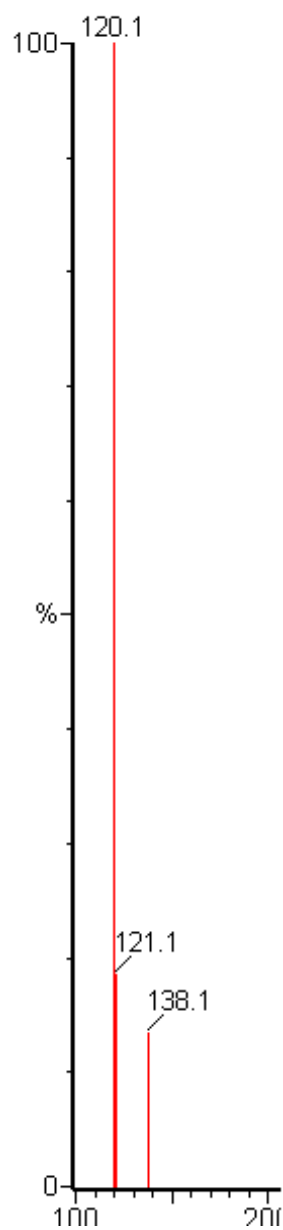
A: Mass Spectrum at 25 V



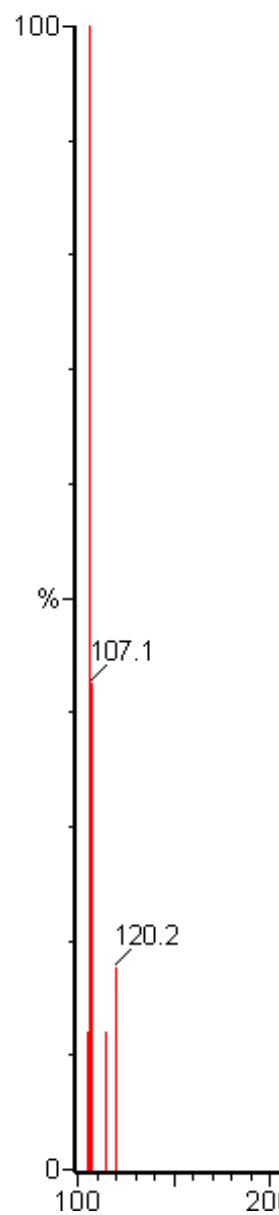
B: Mass Spectrum at 75 V



Appendix 11: Mass Spectra of Unknown Metabolite (**25**) at 25 V and 75 V



A: Mass Spectrum at 25 V



B: Mass Spectrum at 75 V

Appendix 12: Standard HPLC Methods for Normal and Reversed Phase Columns

Reversed Phase Chromatography:

Column: Agilent Eclipse XDB-C18
Size: 4.6mm x 250 mm
Particle: 5 μ m
Flow rate: 1.0 ml/min
Gradient: 50-95% MeOH/0.1% TFA over 20 minutes
UV monitoring: 214nm, 238 nm

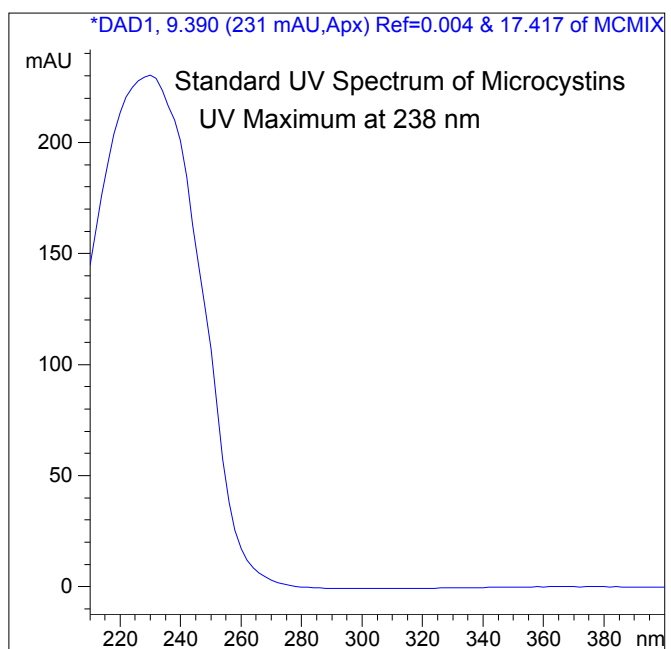
Hydrophilic Liquid Interaction Chromatography:

Column: Tosoh Biosep Amide 80
Size: 2.0mm x 150mm
Particle: 5 μ m
Flow rate: 0.2 ml/min
Gradient:

Time	ACN/ 0.1% FA	Water/ 0.1% FA
0	95	5
13	75	25
13.1	10	90
18	25	75
18.1	65	35
25	35	65

UV monitoring: 214nm, 238nm

Appendix 13: Standard UV Spectrum of Microcystins



Appendix 14: Mass Spectra of Microcystin Standards

